1

Basic Theories and Principles of Nonlinear Beam Deformations

1.1 Introduction

The minimum weight criteria in the design of aircraft and aerospace vehicles, coupled with the ever growing use of light polymer materials that can undergo large displacements without exceeding their specified elastic limit, prompted a renewed interest in the analysis of flexible structures that are subjected to static and dynamic loads. Due to the geometry of their deformation, the behavior of such structures is highly nonlinear and the solution of such problems becomes very complex. The solution complexity becomes immense when flexible structural components have variable cross-sectional dimensions along their length. Such members are often used to improve strength, weight and deformation requirements, and in some cases, architects and planners are using variable cross-section members to improve the architectural aesthetics and design of the structure.

In this chapter, the well known theory of *elastica* is discussed, as well as the methods that are used for the solution of the elastica. In addition, the solution of flexible members of uniform and variable cross-section is developed in detail. This solution utilizes equivalent pseudolinear systems of constant cross-section, as well as equivalent simplified nonlinear systems of constant cross-section. This approach simplifies a great deal the solution of such complex problems. See, for example, Fertis [2, 3, 5, 6], Fertis and Afonta [1], and Fertis and Lee [4].

This chapter also includes, in a brief manner, important historical developments on the subject and the most commonly used methods for the static and the dynamic analysis of flexible members.

1.2 Brief Historical Developments Regarding the Static and the Dynamic Analysis of Flexible members

By looking into past developments on the subject, we observe that the static analysis of flexible members was basically concentrated in the solution of

simple elastica problems. By the term *elastica*, we mean the determination of the exact shape of the deflection curve of a flexible member. This task was carried out by using various types of analytical (closed-form) methods and techniques, as well as various kinds of numerical methods of analysis, such as the finite element method. Numerical procedures were also extensively used to carry out the complicated mathematics when analytical methods were used.

The dynamic analysis of flexible members was primarily concentrated in the computation of their free frequencies of vibration and their corresponding mode shapes. The mode shapes were, one way or another, associated with large amplitudes. In other words, since the free vibration of a flexible member is taking place with respect to its static equilibrium position, we may have large static amplitudes associated with the static equilibrium position and small vibration amplitudes that take place about the static equilibrium position of the flexible member. We may also have large vibration amplitudes that are nonlinearly connected to the static equilibrium position of the member. This gives some fair idea about the complexity of both static and dynamic problems which are related with flexible member.

A brief history of the research work associated with the static and the dynamic analysis of flexible members is discussed in this section. Since the member, in general, can be subjected to both elastic and inelastic behavior, both aspects of this problem are considered.

The deformed configuration for a uniform flexible cantilever beam loaded with a concentrated load P at its free end is shown in Fig. 1.1a. The free-body diagram of a segment of the beam of length x_o is shown in Fig. 1.1b. Note the difference in length between the projected length x in Fig. 1.1a, or Fig. 1.1b, and the length x_o along the length of the member. The importance of such lengths, as well as the other items in the figure, are explained in detail later in this chapter and in following chapters of the book.

The basic equation that relates curvature and bending moment in its general sense was first derived by the brothers, Jacob and Johann Bernoulli, of the well-known Bernoulli family of mathematicians. In their derivation, however, the constant of proportionality was not correctly evaluated. Later on, by following a suggestion that was made by Daniel Bernoulli, L. Euler (1707–1783) rederived the differential equation of the deflection curve and proceeded with the solution of various problems of the elastica [7–10]. J.L. Lagrange (1736–1813) was the next person to investigate the elastica by considering a uniform cantilever strip with a vertical concentrated load at its free end [8, 10–12]. G.A.A. Plana (1781–1864), a nephew of Lagrange, also worked on the elastica problem [13] by correcting an error that was made in Langrange's investigation of the elastica. Max Born also investigated the elastica by using variational methods [14].

Since Bernoulli, many mathematicians, scientists, and engineers researched this subject, and many publications may be found in the literature. The methodologies used may be crudely categorized as either *analytical* (closed-form), or based on *finite element* techniques. The analytical approaches are

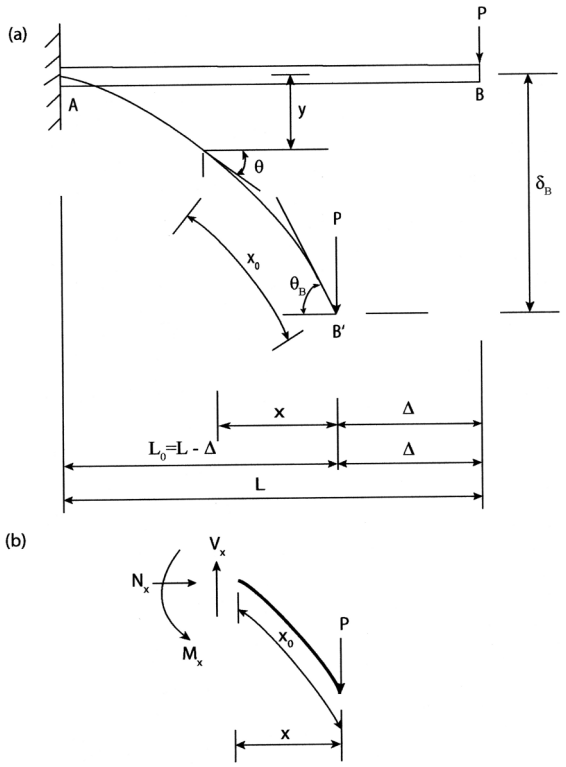

Fig. 1.1. (**a**) Large deformation of a cantilever beam of uniform cross section. (**b**) Free-body diagram of a beam element

based on the Euler–Bernoulli law, while in the finite element method the purpose is to develop a procedure that permits the solution of complex problems in a straightforward manner.

The more widely used analytical methods include *power series, complete and incomplete elliptic integrals*, numerical procedures using the fourth order *Runge–Kutta method*, and the author's method of the *equivalent systems* which utilizes *equivalent pseudolinear systems* and *simplified nonlinear equivalent systems*.

In the *power series* method, the basic differential equation is expressed with respect to x_o, i.e.

$$\frac{d\theta}{dx_0} = \frac{M}{E_1 I_1 f(x_0) g(x_0)} \tag{1.1}$$

where $f(x_o)$ and $g(x_o)$ represent the variation of the moment of inertia $I(x_o)$ and the modulus of elasticity $E(x_o)$, respectively, with respective reference values I_1 and E_1, respectively. Note that for uniform members and linearly elastic materials we have $f(x_o) = g(x_o) = 1.00$. Also note that θ is the angular rotation along the deformed length of the member as shown in Fig. 1.1a.

For constant E, Eq. (1.1) is usually expressed in terms of the shear force V_{x_0} as follows:

$$EI_1 \frac{d}{dx_0}\left\{ f(x_0) \frac{d\theta}{dx_0} \right\} = -V_{x_0} \cos\theta \tag{1.2}$$

or, for members of uniform I,

$$EI \frac{d^2\theta}{dx_0^2} = -V_{x_0} \cos\theta \tag{1.3}$$

In order to apply the power series method, we express θ in Eqs. (1.2) and (1.3) as a function of x_o by using the following Maclaurin's series:

$$\theta(x_0) = \theta(c) + (x_0 - c)\,\theta'(c) + \frac{(x_0 - c)^2}{2!}\theta''(c) + \frac{(x_0 - c)^3}{3!}\theta'''(c) + \cdots \tag{1.4}$$

where c is any arbitrary point along the arc length of the flexible member.

The difficulties associated with the utilization of power series is that for variable stiffness members subjected to multistate loadings, θ depends on both x and x_o. The coordinates x and x_o are defined as shown in Fig. 1.1.

The *method of elliptic integrals* so far is used for simple beams of uniform E and I that are loaded only with concentrated loads. For a uniform beam that is loaded with either a concentrated axial, or a concentrated lateral load, the governing differential equation is of the form

$$\frac{d^2\theta}{dx_0^2} = K\Gamma(\theta) \tag{1.5}$$

where K is an arbitrary constant, and $\Gamma(\theta)$ is a linear combination of $\cos\theta$ and $\sin\theta$. The nonlinear differential equation given by Eq. (1.5) may be integrated by using the elliptic integral method, which requires some certain knowledge of elliptic integrals. The difficulty associated with this method is that it cannot be applied to flexible members with distributed loads, or to flexible members with variable stiffness.

In the *fourth order Runge–Kutta method* the nonlinear differential equations are given in terms of the rotation θ, as shown by Eqs. (1.2) and (1.3). The difficulty associated with this method is that for multistate loadings the expressions for the bending moment involve integral equations which are functions of the large deformation. In such cases, the application of the Runge–Kutta method becomes extremely difficult. However, if θ is only a function of x_o, then the method can be easily applied.

The *method of the equivalent systems*, which was developed initially by the author and his collaborators in order to simplify the solution of complicated linear statics and dynamics problems [5,6,15–30], was extended by the author and his students during the past fifteen years for the solution of nonlinear statics and dynamics problems [1–3, 5, 6, 31–51]. Both elastic and inelastic ranges are considered, as well as the effects of axial compressive forces in both

ranges. The solution of the nonlinear problem is given in the form of *equivalent pseudolinear systems*, or *simplified equivalent nonlinear systems*, which permit very accurately and rather conveniently the solution of extremely complicated nonlinear problems. A great deal of this work is included in this text. Once the pseudolinear system is derived, linear analysis may be used to solve it because its static or dynamic response is identical, or very closely identical, to that of the original complex nonlinear problem. For very complex nonlinear problems, it was found convenient to derive first a simplified nonlinear equivalent system, and then proceed with pseudolinear analysis. Much of this work is included in this text in detail and with application to practical engineering problems.

We continue the discussion with the research by K.E. Bisshoppe and D.C. Drucker [52]. These two researchers used the power series method to obtain a solution for a uniform cantilever beam, which was loaded (1) by a concentrated load at its free end, and (2) by a combined load consisting of a uniformly distributed load in combination with a concentrated load at the free end of the member. J.H. Lau [53] also investigated the flexible uniform cantilever beam loaded with the combined loading, consisting of a uniformly distributed load along its span and a concentrated load at its free end, by using the power series method. He proved that superposition does not apply to large deflection theory, and he plotted some load–deflection curves for engineering applications. P. Seide [54] investigated the large deformation of an extensional simply supported beam loaded by a bending moment at its end, and he found that reasonable results are obtained by the linear theory for relatively large rotations of the loaded end.

Y. Goto et al. [55] used elliptic integrals to derive a solution for plane elastica with axial and shear deformations. H.H. Denman and R. Schmidt [56] solved the problem of large deflection of thin elastica rods subjected to concentrated loads by using a Chebyshev approximation method. The finite difference method was used by T.M. Wang, S.L. Lee, and O.C. Zienkiewicz [57] to investigate a uniform simply supported beam subjected (1) to a nonsymmetrical concentrated load and (2) to a uniformly distributed load over a portion of its span.

The Runge–Kutta and Gill method, in combination with Legendre Jacobi forms of elliptic integrals of the first and second kind, was used by A. Ohtsuki [58] to analyze a thin elastic simply supported beam under a symmetrical three-point bending. The Runge–Kutta method was also used by B.N. Rao and G.V. Rao [59] to investigate the large deflection of a cantilever beam loaded by a tip rotational load. K.T. Sundara Raja Iyengar [60] used the power series method to investigate the large deformation of a simply supported beam under the action of a combined loading consisting of a uniformly distributed load and a concentrated load at its center. At the supports he considered (1) the reactions to be vertical, and (2) the reactions to be normal to the deformed beam by including frictional forces. He did not obtain numerical results. He only developed the equations.

G. Lewis and F. Monasa [61] investigated the large deflection of a thin cantilever beam made out of nonlinear materials of the Ludwick type, and C. Truesdall [62] investigated a uniform cantilever beam loaded with a uniformly distributed vertical load. R. Frisch-Fay in his book *Flexible Bars* [63] solved several elastica problems dealing with uniform cantilever beams, uniform bars on two supports and initially curved bars of uniform cross section, under point loads. He used elliptic integrals, power series, the principle of elastic similarity, as well as Kirchhoff's dynamical analogy to solve such problems.

Researchers such as J.E. Boyd [64], H.J. Barton [65], F.H. Hammel, and W.B. Morton [66], A.E. Seames and H.D. Conway [67], R. Leibold [68], R. Parnes [69], and others also worked on such problems. In all the studies described above, with the exception of the research performed by the author and his collaborators, analytical approaches which include arbitrary stiffness variations and arbitrary loadings, were not treated. This is attributed to the difficulties involved in solving the nonlinear differential equations involved. These subjects, by including elastic, inelastic, and vibration analysis, as well as cyclic loadings, are treated in detail by the author, as stated earlier in this section, and much of this work is included in this text and the references at the end of the text.

Because of the difficulties involved in solving the nonlinear differential equations, most of the early investigators turned their efforts to the utilization of the finite element method to obtain solutions. However, in the utilization of the finite element method, difficulties were developed, as stated earlier, regarding the representation of rigid body motions of oriented bodies subjected to large deformations.

K.M. Hsiao and F.T. Hou [70] used the small deflection beam theory, by including the axial force, to solve for the large rotation of frame problems by assuming that the strains are small. The total stiffness matrix was formulated by superimposing the bending, geometric, and linear beam stiffness matrices. An incremental iterative method based on the Newton–Raphson method, combined with a constant arc length control method, was used for the solution of the nonlinear equilibrium equations.

Y. Tada and G. Lee [71] adopted nodal coordinates and direction cosines of a tangent vector regarding the deformed configuration of elastic flexible beams. The stiffness matrices were obtained by using the equations of equilibrium and Galerkin's method. Their method was applied to a flexible cantilever beam loaded at the free end. T.Y. Yang [72] proposed a matrix displacement formulation for the analysis of elastica problems related to beams and frames. A. Chajes [73] applied the linear and nonlinear incremental methods, as well as the direct method, to investigate the geometrically nonlinear behavior of elastic structures. The governing equations were derived for each method, and a procedure outline was provided regarding the plotting of the load–deflection curves. R.D. Wood and O.C. Zienkiewicz [74] used a continuum mechanics approach with a Lagrangian coordinate system and isoparametric element

for beams, frames, arches, and axisymmetric shells. The Newton–Raphson method was used to solve the nonlinear equilibrium equations.

Some considerable research work was performed on nonlinear vibration of beams. D.G. Fertis [2, 3, 5] and D.G. Fertis and A. Afonta [39, 40] applied the method of the equivalent systems to determine the free vibration of variable stiffness flexible members. D.G. Fertis [2, 3], and D.G. Fertis and C.T. Lee [38, 41, 48] developed a method to be used for the nonlinear vibration and instabilities of elastically supported beams with axial restraints. They have also provided solutions for the inelastic response of variable stiffness members subjected to cyclic loadings. D.G. Fertis [49, 51] used equivalent systems to determine the inelastic vibrations of prismatic and nonprismatic members as well as the free vibration of flexible members.

S. Wionowsky-Krieger [75] was the first one to analyze the nonlinear free vibration of hinged beams with an axial force. G. Prathap [76] worked on the nonlinear vibration of beams with variable axial restraints, and G. Prathap and T.K. Varadan [77] worked on the large amplitude vibration of tapered clamped beams. They used the actual nonlinear equilibrium equations and the exact nonlinear expression for the curvature. C. Mei and K. Decha-Umphai [78] developed a finite element approach in order to evaluate the geometric nonlinearities of large amplitude free- and forced-beam vibrations. C. Mei [79], D.A. Evensen [80], and other researchers worked on nonlinear vibrations of beams.

Analytical research work regarding the inelastic behavior of flexible structures is very limited. D.G. Fertis [2, 3, 49] and D.G. Fertis and C.T. Lee [2–4, 47, 49] did considerable research work on the inelastic analysis of flexible bars using simplified nonlinear equivalent systems, and they have studied the general inelastic behavior of both prismatic and nonprismatic members. G. Prathap and T.K. Varadan [81] examined the inelastic large deformation of a uniform cantilever beam of rectangular cross section with a concentrated load at its free end. The material of the beam was assumed to obey the stress–strain law of the Ramberg–Osgood type. C.C. Lo and S.D. Gupta [82] also worked on the same problem, but they used a logarithmic function of strains for the regions where the material was stressed beyond its elastic limit.

F. Monasa [83] considered the effect of material nonlinearity on the response of a thin cantilever bar with its material represented by a logarithmic stress–strain function. Also J.G. Lewis and F. Monasa investigated the large deflection of thin uniform cantilever beams of inelastic material loaded with a concentrated load at the free end. Again the stress–strain law of the material was represented by Ludwick relation.

In the space age we are living today, much more research and development is needed on these subjects in order to meet the needs of our present and future high technology developments. The need to solve practical nonlinear problems is rapidly growing. Our structural needs are becoming more and more nonlinear. I hope that the work in this text would be of help.

The problem of inelastic vibration received considerable attention by many researchers and practicing engineers. Bleich [86], and Bleich and Salvadory [87], proposed an approach based on normal modes for the inelastic analysis of beams under transient and impulsive loads. This approach is theoretically sound, but it can be applied only to situations where the number of possible plastic hinges is determined beforehand, and where the number of load reversals is negligible. Baron et al. [88], and Berge and da Deppo [89], solved the required equation of motion by using methods that are based on numerical integration. This, however, involved concentrated kink angles which are used to correct for the amount by which the deflection of the member surpasses the actual elastic–plastic point. The methodology is simple, but the actual problem may become very complicated because multiple correction angles and several hinges may appear simultaneously. Lee and Symonds [90], have proposed the method of rigid plastic approximation for the deflection of beams, which is valid only for a single possible yield with no reversals. Toridis and Wen [91], used lumped mass and flexibility models to determine the response of beams.

In all the models developed in the above references, the precise location of the point of reversal of loading is very essential. A hysteretic model where the location of the loading reversal point is not required and where the reversal is automatically accounted for, was first suggested by Bonc [92] for a spring-mass system, and it was later extended by Wen [93] and by Iyender and Dash [94]. In recent years Sues et al. [95] have provided a solution for a single degree of freedom model for degrading inelastic model. This work was later extended by Fertis [2, 3] and Fertis and Lee [38], and they developed a model that adequately describes the dynamic structural response of variable and uniform stiffness members subjected to dynamic cyclic loadings. In their work, the material of the member can be stressed well beyond its elastic limit, thus causing the modulus E to vary along the length of the member. The derived differential equations take into consideration the restoring force behavior of such members by using appropriate hysteretic restoring force models.

The above discussion, is not intended to provide a complete historical treatment of the subject, and the author wishes to apologize for any unintentional omission of the work of other investigators. It provides, however, some insight regarding the state of the art and how the ideas regarding these very important subjects have been initiated.

1.3 The Euler–Bernoulli Law of Linear and Nonlinear Deformations for Structural Members

From what we know today, the first public work regarding the large deformation of flexible members was given by L. Euler (1707–1783) in 1744, and it was continued in the appendix of his well known book *Des Curvis Elastics* [7]. According to Euler, when a member is subjected to bending, we cannot neglect

the slope of the deflection curve in the expression of the curvature unless the deflections are small. Euler has published about 75 substantial volumes, he was a dominant figure during the 18th century, and his contributions to both pure and applied mathematics made him worthy of inclusion in the short list of giants of mathematics – Archimedes (287–212 BC), I. Newton (1642–1727), and C. Gauss (1777–1855).

We should point out, however, that the development of this theory took place in the 18th century, and the credits for this work should be given to Jacob Bernoulli (1654–1705), his younger brother Johann Bernoulli (1667–1748), and Leonhard Euler (1707–1783). Both Bernoulli brothers have contributed heavily in the mathematical sciences and related areas. They also worked on the mathematical treatment of the Greek problems of *isochrone, brahistochrone, isoperimetric figures*, and *geodesies*, which led to the development of the new calculus known as the *calculus of variations*. Jacob also introduced the word *integral* in suggesting the name *calculus integrals*. G.W. Leibniz (1646–1716) used the name *calculus summatorius* for the inverse of the *calculus differentialis*.

The Euler–Bernoulli law states that the bending moment M is proportional to the change in the curvature produced by the action of the load. This law may be written mathematically as follows:

$$\frac{1}{r} = \frac{d\theta}{dx_0} = \frac{M}{EI} \tag{1.6}$$

where r is the radius of curvature, θ is the slope at any point x_o, where x_o is measured along the arc length of the member as shown in Fig. 1.1a, E is the modulus of elasticity, and I is the cross-sectional moment of inertia.

Figure 1.1a depicts the large deformation configuration of a uniform flexible cantilever beam, and Fig. 1.1b illustrates the free-body diagram of a segment of the beam of length x_o. Note the difference in length size between x and x_o in Fig. 1.1b. For small deformations we usually assume that $x = x_o$. For small deformations we can also assume that $L = L_o$ in Fig. 1.1a, because under this condition the horizontal displacement Δ of the free end B of the cantilever beam would be small.

In rectangular x, y coordinates, Eq. (1.6) may be written as

$$\frac{1}{r} = \frac{y''}{\left[1 + (y')^2\right]^{3/2}} = -\frac{M}{EI} \tag{1.7}$$

where

$$y' = \frac{dy}{dx} \tag{1.8}$$

$$y'' = \frac{d^2y}{dx^2} \tag{1.9}$$

and y is the vertical deflection at any x. We also know that

$$y' = \tan\theta \quad \text{or} \quad \theta = \tan^{-1} y' \tag{1.10}$$

Equation (1.7) is a second order nonlinear differential equation, and its exact solution is very difficult to obtain. This equation shows that the deflections are no longer a linear function of the bending moment, or of the load, which means that the principle of superposition does not apply. The consequence is that every case that involves large deformations must be solved separately, since combinations of load types already solved cannot be superimposed. The consequences become more immense when the stiffness EI of the flexible member varies along the length of the member. We discuss this point of view in greater detail, with examples, later in this chapter.

When the deformation of the member is considered to be small, $y\prime$ in Eq. (1.7) is small compared to 1, and it is usually neglected. On this basis, Eq. (1.7) is transformed into a second order linear differential equation of the form

$$\frac{1}{r} = y'' = -\frac{M}{EI} \tag{1.11}$$

The great majority of practical applications are associated with small deformations and, consequently, reasonable results may be obtained by using Eq. (1.11). For example, if $y\prime = 0.1$ in Eq. (1.7), then the denominator of this equation becomes

$$\left[1 + (0.1)^2\right]^{3/2} = 0.985 \tag{1.12}$$

which suggests that we have an error of only 1.52% if Eq. (1.11) is used.

1.4 Integration of the Euler–Bernoulli Nonlinear Differential Equation

Figure 1.2 depicts the large deformation configuration of a tapered flexible cantilever beam loaded with a concentrated vertical load P at its free end. In this figure, y is the vertical deflection of the member at any x, and θ is its rotation at any x. We also have the relations

$$y' = \frac{dy}{dx} \tag{1.13}$$

$$y'' = \frac{d^2y}{dx} \tag{1.14}$$

and

$$y' = \tan\theta \quad \text{or} \quad \theta = \tan^{-1} y' \tag{1.15}$$

In rectangular x, y coordinates, the Euler–Bernoulli law for large deformation produced by bending may be written as [2,3] (see also Eq. (1.7):

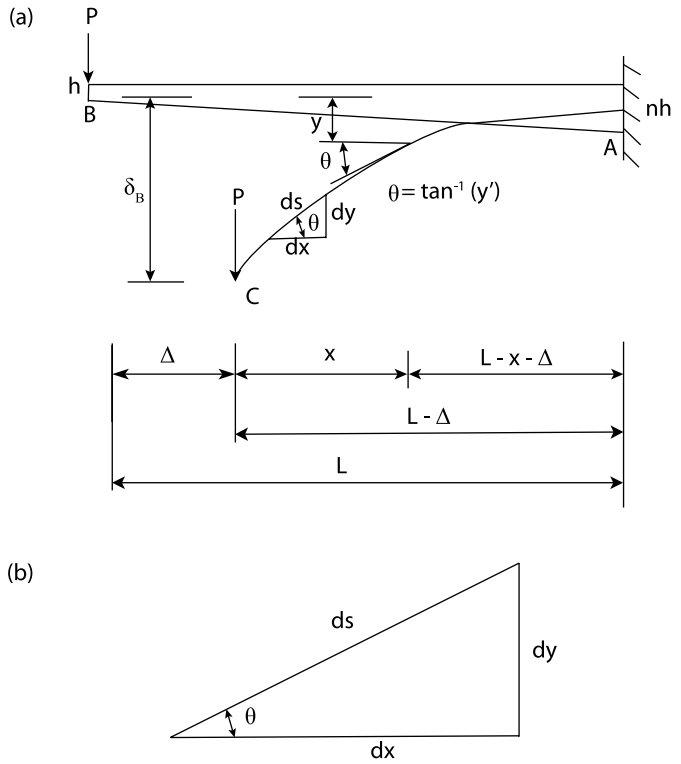

Fig. 1.2. (**a**) Tapered flexible cantilever beam loaded with a vertical concentrated load P at the free end. (**b**) Infinitesimal beam element

$$\frac{y''}{\left[1+(y')^2\right]^{3/2}} = -\frac{M_x}{E_x I_x} \tag{1.16}$$

where M_x is the bending moment produced by the loading on the beam. E_x is the modulus of elasticity of its material, and I_x is its cross-sectional moment of inertia.

Since the loading on the beam can be arbitrary and E_x and I_x can be variable, we may rewrite Eq. (1.16) in a more general form as follows:

$$\frac{y''}{\left[1+(y')^2\right]^{3/2}} = -\frac{M_x}{E_1 I_1 f(x)\, g(x)} \tag{1.17}$$

where f(x) is the moment of inertia function representing the variation of I_x with I_1 as a reference value, and g(x) is the modulus function representing the variation of E_x with E_1 as a reference value. If E and I are constant, then $g(x) = f(x) = 1.00$.

We integrate Eq. (1.17) by making changes in the variables. We let $y' = p$ and then $y'' = p'$. Thus, from Eq. (1.16), we obtain

$$\frac{p'}{\left[1 + p^2\right]^{3/2}} = \lambda(x) \tag{1.18}$$

where

$$\lambda(x) = \frac{M_x}{E_x I_x} \tag{1.19}$$

Now we rewrite Eq. (1.18) as follows:

$$\frac{dp/dx}{\left[1 + p^2\right]^{3/2}} = \lambda(x) \tag{1.20}$$

By multiplying both sides of Eq. (1.20) by dx and integrating once, we find

$$\int \frac{dp}{\left[1 + p^2\right]^{3/2}} = \int \lambda(x)\, dx \tag{1.21}$$

We can integrate Eq. (1.21) by making the following substitutions:

$$p = \tan\theta \tag{1.22}$$

$$dp = \sec^2\theta\, d\theta \tag{1.23}$$

By using the beam element shown in Fig. 1.2b and applying the Pythagorean theorem, we find

$$(ds)^2 = (dx)^2 + (dy)^2 \quad \text{or} \quad ds = \left[(dx)^2 + (dy)^2\right]^{1/2} \tag{1.24}$$

$$\begin{aligned} \frac{ds}{dx} = \left[1 + \left(\frac{dy}{dx}\right)^2\right]^{1/2} &= \left[1 + (\tan\theta)^2\right]^{1/2} \\ &= \left[1 + p^2\right]^{1/2} \end{aligned} \tag{1.25}$$

Thus,

$$\cos\theta = \frac{dx}{ds} = \frac{1}{\left[1 + p^2\right]^{1/2}} \tag{1.26}$$

and from Eq. (1.22), we find

$$\sin\theta = p\cos\theta = \frac{p}{\left[1 + p^2\right]^{1/2}} \tag{1.27}$$

By substituting Eqs. (1.22) and (1.23) into Eq. (1.21) and also making use of Eqs. (1.26) and (1.27), we find

$$\int \frac{\sec^2\theta \; d\theta}{\left[1+\frac{\sin^2\theta}{\cos^2\theta}\right]^{3/2}} = \int \lambda\,(x)\,dx \tag{1.28}$$

or, by performing trigonometric manipulations, Eq. (1.28) reduces to the following equation:

$$\int \cos\theta \; d\theta = \int \lambda\,(x)\,dx \tag{1.29}$$

Integration of Eq. (1.29), yields

$$\sin\theta = \varphi\,(x) + C \tag{1.30}$$

where the function $\varphi(x)$ represents the integration of $\lambda(x)$.

Equation (1.30) may be rewritten in terms of p and y' by using Eq. (1.27). Thus,

$$\frac{p}{\left[1+p^2\right]^{1/2}} = \varphi\,(x) + C \tag{1.31}$$

$$\frac{y'}{\left[1+(y')^2\right]^{1/2}} = \varphi\,(x) + C \tag{1.32}$$

where C is the constant of integration which can be determined from the boundary conditions of the given problem. If we will solve Eq. (1.32) for $y'(x)$, we obtain the following equation:

$$y'\,(x) = \frac{\varphi\,(x) + C}{\sqrt{1-[\varphi\,(x)+C]^2}} \tag{1.33}$$

Integration of Eq. (1.33) yields the large deflection y(x) of the member. Thus,

$$y\,(x) = \int_0^x \frac{\varphi\,(\eta) + C}{\sqrt{1-[\varphi\,(\eta)+C]^2}} d\eta \tag{1.34}$$

This shows that when M_x/E_xI_x is known and it is integrable, then the Euler–Bernoulli equation may be solved directly for $y'(x)$ as illustrated in the solution of many flexible beam problems in [2, 3]. In the same references, utilization of pseudolinear equivalent systems is made, which simplify a great deal the solution of such problems. A numerical integration may be also used for Eq. (1.34), or Eq. (1.16), by using the Simpson's rule discussed in the following section of this text.

1.5 Simpson's One-Third Rule

Simpson's one-third rule is one of the most commonly used numerical method to approximate integration. It is used primarily for cases where exact integration is very difficult or impossible to obtain. Consider, for example, the integral

$$\delta = \int_a^b f(x)\,dx \tag{1.35}$$

between the limits a and b. If we divide the integral between the limits x=a and x=b into n equal parts, where n is an even number, and if $y_0, y_1, y_2, \ldots, y_{n-1}, y_n$ are the ordinates of the curve $y = f(x)$, as shown in Fig. 1.3, then, according to Simpson's one-third rule we have

$$\int_a^b f(x)\,dx = \frac{\lambda}{3}\left(y_0 + 4y_1 + 2y_2 + 4y_3 + \cdots + 2y_{n-2} + 4y_{n-1} + y_n\right) \tag{1.36}$$

where

$$\lambda = \frac{b-a}{n} \tag{1.37}$$

Simpson's rule provides reasonably accurate results for practical applications.

Let it be assumed that it is required to determine the value δ of the integral

$$\delta = \int_0^L x^2 dx \tag{1.38}$$

We divide the length L into 10 equal segments, yielding $\lambda = 0.1L$. By applying Simpson's rule given by Eq. (1.36), and noting that $y = f(x) = x^2$, we find

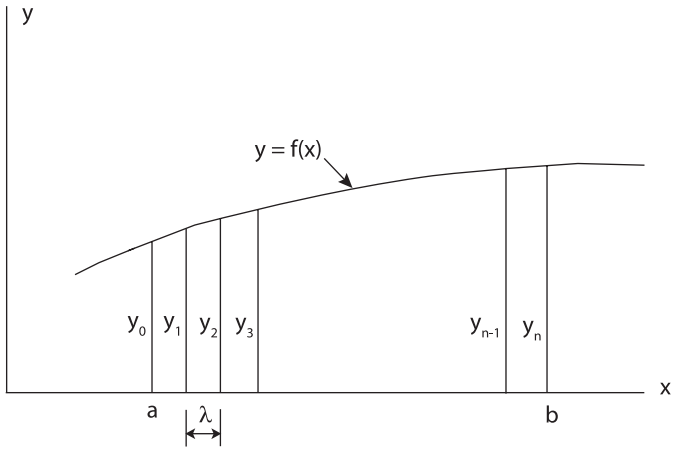

Fig. 1.3. Plot of a function $y = f(x)$

$$\delta = \frac{0.1L}{3}\Big[(1)(0)^2 + (4)(0.1)^2 + (2)(0.2)^2 + (4)(0.3)^2 + (2)(0.4)^2 + (4)(0.5)^2 + (2)(0.6)^2 + (4)(0.7)^2 + (2)(0.8)^2 + (4)(0.9)^2 + (1)(1)^2\Big] L^2 = \frac{L^3}{3}$$

Note that for $\lambda = 0.1L$, the values of f(x) are $y_o = (0)^2$, $y_1 = (0.1L)^2$, $y_2 = (0.2L)^2$, and so on. In this case, the exact value of the integral is obtained.

As a second example, let it be assumed that it is required to find the value δ of the integral

$$\delta = \int_0^L x^3 dx \tag{1.39}$$

Again, we subdivide the length L into 10 equal segments, yielding $\lambda = 0.1L$. In this case, the Simpson's one-third rule yields

$$\delta = \frac{0.1L}{3}\Big[(1)(0)^3 + (4)(0.1)^3 + (2)(0.2)^3 + (4)(0.3)^2 + (2)(0.4)^3 + (4)(0.5)^3 + (2)(0.6)^3 + (4)(0.7)^3 + (2)(0.8)^3 + (4)(0.9)^3 + (1)(1)^3\Big] L^3 = \frac{0.75L^4}{3} = \frac{L^4}{4}$$

The exact value of the integral is obtained again in this case.

More complicated integrals may be also evaluated in a similar manner, as shown later in this text. For example, let it be assumed that it is required to determine the length L of a flexible bar given by the integral

$$L = \int_0^{840} \left[1 + (y')^2\right]^{1/2} dx \tag{1.40}$$

where

$$y'(x) = \frac{G(x)}{\left\{1 - [G(x)]^2\right\}^{1/2}} \tag{1.41}$$

and

$$G(x) = 1.111(10)^{-6} x^2 - 0.783922 \tag{1.42}$$

Equation (1.40) is an extremely important equation in nonlinear mechanics for the analysis of flexible bars subjected to large deformations [2,3]. It relates the length L of the bar with the slope y' at points along its deformed shape.

For illustration purposes, we use here n=10, and from Eq. (1.37) we obtain

$$\lambda = \frac{840 - 0}{10} = 84$$

From Eq. (1.40), we note that

$$f(x) = \left[1 + (y')^2\right]^{1/2} \tag{1.43}$$

The values of f(x) at x = 0, 84, 168, ..., 840 are designated as $y_o, y_1, y_2, \ldots, y_{10}$, respectively, and they are obtained by using Eq. (1.43) in conjunction with Eqs. (1.42) and (1.41). For example, for x=0, we have

$$G(0) = -0.783922$$
$$y'(0) = \frac{-0.783922}{\sqrt{1-(-0.783922)^2}} = -1.262641$$
$$y_0 = f(0) = \sqrt{1+(-1.262641)^2} = 1.610671$$

For x=84 in., we have

$$G(84) = 1.111\,(10)^6\,(84)^2 - 0.783922 = 0.776083$$
$$y'(84) = \frac{-0.776083}{\sqrt{1-(-0.776083)^2}} = -1.230645$$
$$y_1 = f(84) = \sqrt{1+(-1.230645)^2} = 1.585713$$

In a similar manner, the remaining points $y_2, y_3, \ldots, y_{10}$, can be determined. On this basis, Eq. (1.36) yields

$$\begin{aligned} L = \frac{84}{3}\,&[1.610671 + (4)\,(1.585713) + (2)\,(1.518561) + (4)\,(1.426963) \\ &+ (2)\,(1.328753) + (4)\,(1.236242) + (2)\,(1.156021) + (4)\,(1.090986) \\ &+ (2)\,(1.042370) + (4)\,(1.011280) + 1] \\ = \frac{84}{3}\,&(38.106817) = 1,067\,\text{in.} \end{aligned}$$

It should be realized that the value obtained for L is an approximate one, but better accuracy can be obtained by using larger values for the parameter n in Eq. (1.37). For practical applications, however, the design engineer usually has a fair idea about their accuracy requirements, and satisfactory and safe designs can be obtained by using approximate solutions.

1.6 The Elastica Theory

The exact shape of the deflection curve of a flexible member is called the elastica. The most popular elastica problem is the solution of the flexible uniform cantilever beam loaded with a concentrated load P at the free end, as shown in Fig. 1.1a.

The large deformation configuration of this cantilever beam caused by the vertical load P is shown in Fig. 1.2a. Note that the end point B moved to

point C during the large displacement of point B. The beam is assumed to be inextensible and, consequently, the arc length AC of the deflection curve is equal to the initial length AB. We also assumed that the vertical load P remained vertical during the deformation of the member.

The expression for the bending moment M_x at any $0 \leq x \leq L_o$ may be obtained by using the free-body diagram in Fig. 1.1b and applying statics, i.e.,

$$M_x = -Px \tag{1.44}$$

In rectangular coordinates, the Euler–Bernoulli equation is given by Eq. (1.16), That is,

$$\frac{y''}{\left[1 + (y')^2\right]^{3/2}} = -\frac{M_x}{E_x I_x} \tag{1.45}$$

where E_x is the modulus of elasticity along the length of the member, and I_x is the moment of inertia at cross sections along its length. By substituting Eq. (1.44) into Eq. (1.45) and assuming that E and I are uniform, we obtain

$$\frac{y''}{\left[1 + (y')^2\right]^{3/2}} = \frac{Px}{EI} \tag{1.46}$$

Equation (1.45) may be also expressed in terms of the arc length x_o by using Eq. (1.6). That is

$$E_{x_0} I_{x_0} \frac{d\theta}{dx_0} = -M_x \tag{1.47}$$

By using Eq. (1.44) and assuming that E and I are constant along the length of the member, we find

$$\frac{d\theta}{dx_0} = \frac{Px}{EI} \tag{1.48}$$

By differentiating Eq. (1.48) once with respect to x_o, we obtain

$$\frac{d^2\theta}{dx_0^2} = \frac{P}{EI} \cos\theta \tag{1.49}$$

By assuming that

$$E_x I_x = E_1 I_1 g(x_0) f(x_0) \tag{1.50}$$

where $g(x_o)$ represents the variation of E_x with respect to a reference value E_1, and $f(x_o)$ represents the variation of I_x, with respect to a reference value I_1, we can differentiate Eq. (1.47) once to obtain

$$\frac{d}{dx_0} \left\{ E_1 I_1 g(x_0) f(x_0) \frac{d\theta}{dx_0} \right\} = -V_{x_0} \cos\theta \tag{1.51}$$

For members of uniform cross section and of linearly elastic material, we have $g(x_o) = f(x_o) = 1.0$.

Equations (1.46) and (1.49) are nonlinear second order differential equations and exact solutions of these two equations are not presently available. Elliptic integral solutions are often used by investigators (see, e.g., Frisch-Fay [63]), but they are very complicated. This problem, as well as many other flexible beam problems, is discussed in detail in later sections of this chapter and other chapters of the book, where convenient methods of analysis are developed by the author and his collaborators to simplify the solution of such very complicated problems.

The integration of Eq. (1.46) may be carried out as discussed in Section 1.4. By using Eqs. (1.19) and (1.44), we write $\lambda(x)$ as follows:

$$\lambda(x) = -\frac{M_x}{EI} = \frac{Px}{EI} \tag{1.52}$$

Thus,

$$\varphi(x) = \int \lambda(x)\, dx = \frac{Px^2}{2EI} \tag{1.53}$$

On this basis, Eq. (1.32) yields

$$\frac{y'}{\left[1 + (y')^2\right]^{1/2}} = \varphi(x) + C$$

or, by substituting for $\varphi(x)$ using Eq. (1.53), we obtain

$$\frac{y'}{\left[1 + (y')^2\right]^{1/2}} = \frac{Px^2}{2EI} + C \tag{1.54}$$

where C is the constant of integration which can be determined by applying the boundary condition of zero y' at $x = L_o = (L - \Delta)$. By using this boundary condition in Eq. (1.54), we find

$$C = -\frac{P(L - \Delta)^2}{2EI} \tag{1.55}$$

By substituting Eq. (1.55) into Eq. (1.54), we obtain

$$\frac{y'}{\left[1 + (y')^2\right]^{1/2}} = G(x) \tag{1.56}$$

where

$$G(x) = \frac{P}{2EI}\left[x^2 - (L - \Delta)^2\right] \tag{1.57}$$

Thus, by solving Eq. (1.56) for y', we obtain

$$y'(x) = \frac{G(x)}{\left\{1 - [G(x)]^2\right\}^{1/2}} \tag{1.58}$$

The same expression could be obtained directly from Eq. (1.33) by substituting for $\varphi(x)$ and C, which are the expressions given by Eqs. (1.53) and (1.55), respectively.

The large deflection y at any $0 \leq x \leq L_o$ may now be obtained by integrating once Eq. (1.58) and satisfying the boundary condition of zero deflection at $x = L_o$ for the evaluation of the constant of integration. It should be noted, however, that G(x) in Eq. (1.57) is a function of the unknown horizontal displacement Δ of the free end of the beam. The value of Δ may be determined from the equation

$$L = \int_0^{L_o} \left[1 + (y')^2\right]^{1/2} dx \tag{1.59}$$

by using a trial-and-error procedure. That is, we assume a value of Δ in Eq. (1.58) and then carry out the integration in Eq. (1.59) to determine the length L of the member. The procedure may be repeated for various values of Δ until the correct length L is obtained. This procedure is explained in detail in the numerical examples at the end of this section, as well as in many other sections of this text.

The integration in Eq. (1.59) becomes in many cases more convenient if we introduce the variable

$$\xi = \frac{x}{L - \Delta} \tag{1.60}$$

$$d\xi = \frac{dx}{L - \Delta} \tag{1.61}$$

On this basis, Eq. (1.59) may be written as

$$L = (L - \Delta) \int_0^1 \left\{1 + [y'(\xi)]^2\right\}^{1/2} d\xi \tag{1.62}$$

or, by using Eqs. (1.57) and (1.58) and the variable ξ, we can write Eq. (1.62) as follows:

$$L = (L - \Delta) \int_0^1 \frac{1}{\left\{1 - [G(\xi)]^2\right\}^{1/2}} d\xi \tag{1.63}$$

where

$$G(\xi) = \frac{P(L - \Delta)^2}{2EI}\left(\xi^2 - 1\right) \tag{1.64}$$

It should be pointed out again here that Eqs. (1.45) and (1.47) are second order nonlinear differential equations which describe the exact shape of the deflection curve of the flexible beam. In conventional applications these equations are linearized by neglecting the square of the slope $(y')^2$ in Eq. (1.45) as being small compared to unity. This assumption is permissible, as stated

earlier, provided that the deflections are very small when they are compared with the length of the beam. For flexible bars, where deflections are large when they are compared with the length of the member, this assumption is not permissible, and Eq. (1.45), or Eq. (1.47), must be used in its entirety. This means that the deflections are no longer a linear function of the bending moment, or of the load, and consequently the principle of superposition does not apply. Therefore, every case involving large deformations has to be solved independently, since combinations of load types already solved cannot be superimposed. The situation yields much greater consequences when the stiffness EI of the member is also variable.

Example 1.1 For the uniform flexible cantilever beam in Fig. 1.1a, determine the rotation θ_B and the horizontal displacement Δ of its free end B. Assume that P = 0.4 kip (1.78 kN), L = 1,000 in. (25.4 m), and EI = 180×10^3 kip in.^{2} (516.54×10^3 N m^2).

Solution: In order to obtain a solution to this problem we can use Eqs. (1.57), (1.58), and (1.54). From Eq. (1.57), by substituting the appropriate values for the stiffness EI of the member and its length L, we find

$$\begin{aligned} G(x) &= \frac{0.4}{(2)(180)(10)^3}\left[x^2 - (1{,}000 - \Delta)^2\right] \\ &= 1.111\,(10)^{-6}\left[x^2 - (1{,}000 - \Delta)^2\right] \end{aligned} \tag{1.65}$$

The horizontal displacement Δ of the free end of the member may be evaluated by applying a trial-and-error procedure using Eq. (1.59).

The trial-and-error procedure may be initiated by assuming values of Δ until we find the one that satisfies Eq. (1.59). For example, if we assume $\Delta = 160$ in. (4.064 m), Eq. (1.65) yields

$$G(x) = 1.111\,(10)^{-6}\,x^2 - 0.783922 \tag{1.66}$$

By using the assumed value for Δ, we find $L_0 = 1{,}000 - 160 = 840$ in. (21.336 m). Therefore,

$$y'(x) = \frac{G(x)}{\left\{1 - [G(x)]^2\right\}^{1/2}} \tag{1.67}$$

$$L = \int_0^{840} \left[1 + (y')^2\right]^{1/2} dx \tag{1.68}$$

where G(x) is as shown by Eq. (1.66).

The integration of Eq. (1.68) may be carried out numerically with sufficient accuracy by using Simpson's rule, as shown in Section 1.5, or by using other known numerical procedures. The Simpson's One-Third rule will be used here.

According to this rule, the integral of Eq. (1.68) may be evaluated from the general equation given by Eqs. (1.36) and (1.37). We rewrite these equation as shown below

$$\int_a^b f(x)\,dx = \frac{\lambda}{3}\left(y_0 + 4y_1 + 2y_2 + 4y_3 + \cdots + 2y_{n-2} + 4y_{n-1} + y_n\right) \quad (1.69)$$

where

$$\lambda = \frac{b-a}{n} \quad (1.70)$$

$y_0, y_1, y_2, \ldots, y_n$ are the ordinates of the curve $y = f(x)$, and n is the number of equal parts we use between the limits $x = a$ and $x = b$.

For illustrative purposes, we use $n = 10$, and from Eq. (1.70) we obtain

$$\lambda = \frac{840-0}{10} = 84$$

From Eq. (1.68), we note that

$$f(x) = \left[1 + (y')^2\right]^{1/2} \quad (1.71)$$

The values of f(x) at $x = 0, 84, 168, \ldots, 840$ are designated as $y_0, y_1, y_2, \ldots, y_{10}$, respectively, and they are obtained by using Eq. (1.71) in conjunction with Eqs. (1.66) and (1.67). For example, for $x = 0$, we have

$$G(0) = -0.783922$$
$$y'(0) = \frac{-0.783922}{\sqrt{1-(-0.783922)^2}} = -1.262641$$
$$y_0 = f(0) = \sqrt{1+(-1.262641)^2} = 1.610671$$

For $x = 84$

$$G(84) = 1.111\,(10)^{-6}\,(84)^2 - 0.783922 = -0.776083$$
$$y'(84) = \frac{-0.776083}{\sqrt{1-(-0.776083)^2}} = -1.230645$$
$$y_1 = f(84) = \sqrt{1+(-1.230645)^2} = 1.585713$$

In a similar manner the remaining points $y_2, y_3, \ldots, y_{10}$ can be determined. On this basis, Eq. (1.69) yields

$$\begin{aligned} L = \frac{84}{3}\,&[1.610671 + (4)(1.585713) + (2)(1.518561) + (4)(1.426963) \\ &+ (2)(1.328753) + (4)(1.236242) + (2)(1.156021) + (4)(1.090986) \\ &+ (2)(1.042370) + (4)(1.011280) + 1] \\ = \frac{84}{3}\,&(38.106817) = 1,067\,\text{in.}\ (27.10\,\text{m}) \end{aligned}$$

Since the actual length L = 1,000 in. (25.4 m), the procedure may be repeated with a new value for Δ. With computer assistance, the correct value of Δ was found to be 183.10 in. (4.65 m).

With known Δ, the value of y' and rotation θ_B at the free end B of the member may be obtained by using Eqs. (1.65), (1.67), and (1.10). From Eq. (1.65), we obtain

$$G(0) = 1.111(10)^{-6}\left[0 - (1{,}000 - 183.10)^2\right] = -0.741399$$

and from Eq. (1.67), we find

$$y'(0) = \frac{-0.741399}{\sqrt{1-(-0.741399)^2}} = \frac{-0.741399}{0.671065} = -1.104810$$

Therefore, from Eq. (1.10), we find

$$\theta_B = \tan^{-1} y'(0) = 47.85^\circ$$

Also, Eq. (1.67), in conjunction with Eq. (1.65), can be used to determine the values of $y'(x)$, and consequently those of θ, at other points x. This procedure is explained in detail in later parts of this text.

The values of θ_B and Δ were also determined by using elliptic integrals. The results obtained are $\theta_B = 47.44^\circ$, and Δ = 181.67 in. (4.61 m).

1.7 Moment and Stiffness Dependence on the Geometry of the Deformation of Flexible Members

To comprehend the various methods and methodologies developed in this text, as well as their application to practical engineering problems, we should realize first that the expressions for the bending moment M_x and the moment of inertia I_x of the flexible member are generally nonlinear functions of the large deformation of the member. These two quantities may be expressed as a function of x and x_o as follows:

$$M_x = M(x, x_0) \tag{1.72}$$

$$I_x = I_1 f(x, x_0) \tag{1.73}$$

where x is the abscissa of center line points of the deformed configuration of the member, x_o is the arc length of the deformed segment, I_1 is the reference moment of inertia, and $f(x, x_o)$ is a function representing the variation of I_x. For visual observation see, for example, Fig. 1.1. On this basis, the Euler–Bernoulli law given by Eq. (1.16) becomes a *nonlinear integral* differential equation that is extremely difficult to solve.

To reduce the complexity of such types of problems, we express the arc length $x_o(x)$ of the flexible member in terms of its horizontal displacement $\Delta(x)$, where $0 \leq x \leq (L - \Delta)$. See Fig. 1.1a or Fig. 1.2a. This is accomplished as follows:

$$x_0(x) = x + \Delta(x) \tag{1.74}$$

We also know, as shown from the discussion of Sect. 1.4, that the expression $x_o(x)$ is an integral function of the deformation and it can be expressed as

$$x_0(x) = \int_0^x \left\{1 + [y'(x)]^2\right\}^{1/2} dx \tag{1.75}$$

The derivation of Eq. (1.74) can be initiated by considering a segment dx_o before and after deformation, as shown in Fig. 1.4. By using the Pythagorean theorem we write

$$[dx_0]^2 = [dx]^2 + [dy]^2 \tag{1.76}$$

If we assume that

$$dx_0 = dx + d\Delta(x) \tag{1.77}$$

and then substitute into Eq. (1.76), we obtain

$$[dx + d\Delta(x)]^2 = [dx]^2 + [dy]^2 \tag{1.78}$$

or

$$dx + d\Delta(x) = \left\{1 + [y'(x)]^2\right\}^{1/2} dx \tag{1.79}$$

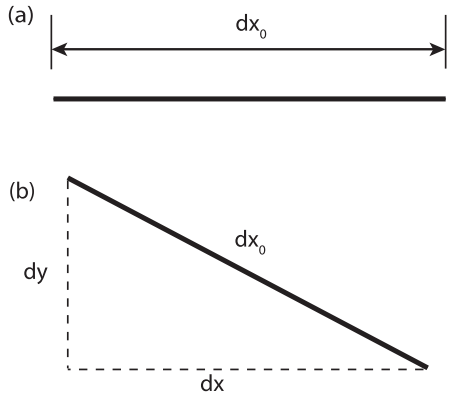

Fig. 1.4. (**a**) Undeformed configuration of an arc length segment dx_o. (**b**) Deformed configuration of dx_o

Integration of Eq. (1.79) with respect to x, yields the expression

$$x + \Delta(x) = \int_0^x \left\{1 + [y'(x)]^2\right\}^{1/2} dx \tag{1.80}$$

This expression provides the same results as Eqs. (1.74) and (1.75).

If we consider flexible members where one of their end supports is permitted to move in the horizontal direction, such as cantilever beams, simply supported beams, etc., approximate expressions for the variation of $\Delta(x)$ may be written and used to facilitate the solution of the nonlinear flexible beam problems. The cases of $\Delta(x)$ that have been investigated by the author and his collaborators and are proven to provide accurate results, are as follows [2, 3]

$$\Delta(x) = \text{constant} = \Delta \tag{1.81}$$

$$\Delta(x) = \Delta \frac{x}{L_0} \tag{1.82}$$

$$\Delta(x) = \Delta \sqrt{\frac{x}{L_0}} \tag{1.83}$$

$$\Delta(x) = \Delta \sin \frac{\pi x}{2L_0} \tag{1.84}$$

where Δ is the horizontal displacement of the movable end, and $L_o = (L - \Delta)$. The plots of the variations of $\Delta(x)$ given by Eqs. (1.81)–(1.84) are shown in Fig. 1.5. We can see from this figure that Δ is an upper limit. Even using Eq. (1.81) which is an upper limit, we obtain reasonably accurate results with error less than 3%. This shows that the variation of the bending moment M_x, and, consequently, the deformation of the member, are largely dependent

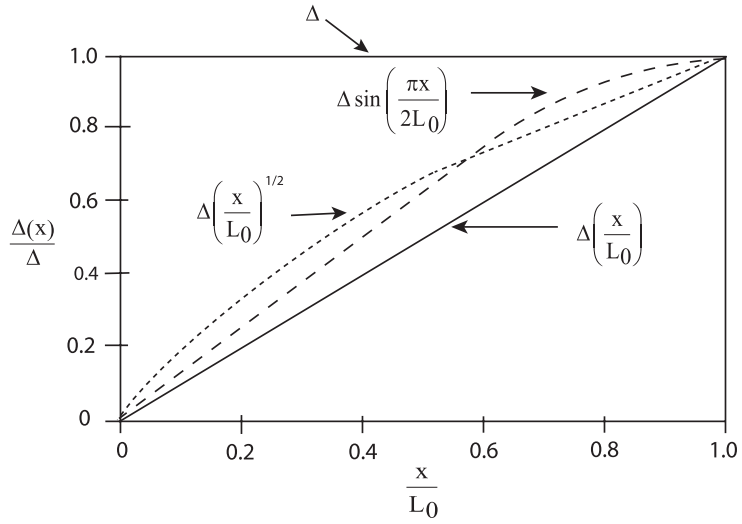

Fig. 1.5. Graphs of various cases of $\Delta(x)$

upon the boundary condition of $\Delta(x)$ at the moving end of the member, and it is rather insensitive to the variation of $\Delta(x)$ between the ends of the member. This is particularly true when the deformations are very large.

The variable moment of inertia I_x of a flexible member, as stated earlier, is a nonlinear function of the deformation. For tapered members that are loaded with concentrated loads only, the variation of the depth h(x) of the member may be approximated by the expression

$$h(x) = (n-1)\left[\frac{1}{n-1} + \frac{x}{L-\Delta}\right] h \tag{1.85}$$

where x is the abscissa of points of the centroidal axis of the member in its deformed configuration, n represents the taper, h is a reference height, and L is the undeformed length of he member. The error of 3% or less associated with the use of Eq. (1.85) is considered small for practical applications. Under this assumption, the solution of flexible members loaded with concentrated loads only, will not require the utilization of integral equations or the use of Eqs. (1.81)–(1.84). This point of view is amply illustrated later.

The following examples illustrate the application of the preceding theory.

Example 1.2 For the tapered flexible cantilever beam shown in Fig. (1.6), derive its exact integral nonlinear differential equation. Also suggest reasonable approximate ways to simplify the complexity of the problem. Assume that the modulus of elasticity E_x is constant and equal to E.

Solution: The Euler–Bernoulli nonlinear differential equation is

$$\frac{y''}{\left[1+(y')^2\right]^{3/2}} = -\frac{M_x}{E_1 I_1 f(x)\, g(x)} \tag{1.86}$$

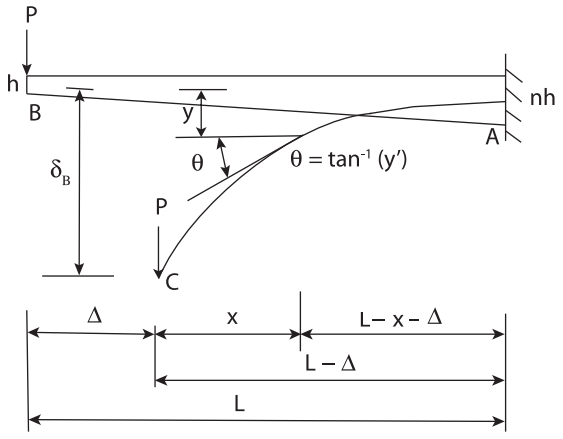

Fig. 1.6. Tapered flexible cantilever beam loaded with a vertical concentrated load P at the free end

where f(x) is the moment of inertia function with moment of inertia I_1 as a reference value, and g(x) represents the variation of E_x with respect to a reference value E_1. In this case we assume that the modulus of elasticity is constant and equal to E, thus making g(x) = 1.

By selecting the moment of inertia I_B at the free end B of the tapered beam as the reference value, the variation of the moment of inertia I_x at any $0 \leq x \leq (L - \Delta)$, where Δ is the horizontal displacement of the free end B, see Fig. 1.6, is written as follows:

$$\begin{aligned} I_x &= \frac{bh^3}{12}\left[f\left(x_0\right)\right] \\ &= I_B\left[1 + \frac{(n-1)}{L}x_0\right]^3 = I_B f\left(x\right) \end{aligned} \tag{1.87}$$

where

$$I_B = \frac{bh^3}{12} \tag{1.88}$$

$$x_0 = \int_0^x \left\{1 + \left[y'\left(x\right)\right]^2\right\}^{1/2} dx \tag{1.89}$$

$$f\left(x\right) = \left[1 + \frac{(n-1)}{L}x_0\right]^3 \tag{1.90}$$

and b is the constant width of the tapered member.

From Fig. 1.6 we observe that the bending moment M_x at any x from the free end C, is given by the expression

$$M_x = -P_x \tag{1.91}$$

By substituting Eqs. (1.87) and (1.91) into Eq. (1.86) and noting that g(x)=1, we find

$$\frac{y''}{\left[1 + \left(y'\right)^2\right]^{3/2}} = \frac{P}{EI_B}\frac{x}{\left\{1 + \frac{(n-1)}{L}\int_0^x \left[1 + \left(y'\left(x\right)\right)^2\right]^{1/2} dx\right\}^3} \tag{1.92}$$

Equation (1.92) is the exact integral nonlinear differential equation representing the given problem and its solution in general, is very complicated. Therefore, reasonable approximation must be used to simplify the problem. A reasonable simplification would be to use the approximate expression for h(x) given by Eq. (1.85). On this basis, by using Eq. (1.85) and applying the well known expression $bh^3(x)/12$ for beam with rectangular cross section, we find

$$I_x = \frac{bh^3}{12}\left[1 + (n-1)\frac{x}{L - \Delta}\right]^3 = I_1 f\left(x\right) \tag{1.93}$$

where

$$I_1 = I_B = \frac{bh^3}{12} \tag{1.94}$$

and

$$f(x) = \left[1 + (n-1)\frac{x}{L-\Delta}\right]^3 \tag{1.95}$$

On this basis, by substituting Eqs. (1.91), (1.94) and (1.95) into Eq. (1.86), we obtain

$$\frac{y''}{\left[1+(y')^2\right]^{3/2}} = \frac{P(L-\Delta)^3}{EI_B}\frac{x}{[(n-1)x+(L-\Delta)]^3} \tag{1.96}$$

Equation (1.96) is the simplified nonlinear differential equation representing the tapered cantilever beam in Fig. 1.6. This equation, as shown later in the text, is far easier to solve compared to Eq. (1.92), and provides accurate results.

Example 1.3 For the uniform flexible cantilever beam loaded with a uniformly distributed load w_o as shown in Fig. 1.7, determine its exact integral nonlinear differential equation. Also suggest reasonable approximate ways to simplify the complexity of the problem. Assume that the modulus of elasticity E_x is constant and equal to E.

Solution: The large deformation configuration of the member is depicted in Fig. 1.7. The bending moment M_x at any distance $0 \leq x \leq L_o$, where $L_o = L - \Delta$, is

$$M_x = -w_0 x_0 \frac{x}{2} \tag{1.97}$$

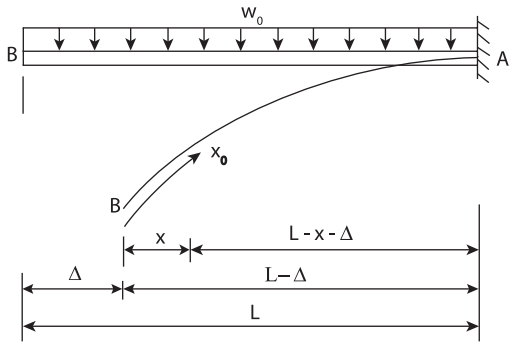

Fig. 1.7. Uniform cantilever beam loaded with a uniformly distributed load w_o over its entire span

From Eq. (1.75) we have

$$x_0 = \int_0^x \left\{1 + [y'(x)]^2\right\}^{1/2} dx \tag{1.98}$$

By substituting Eq. (1.98) into Eq. (1.97), we have

$$M_x = -\frac{w_0 x}{2} \int_0^x \left\{1 + [y'(x)]^2\right\}^{1/2} dx \tag{1.99}$$

By substituting Eq. (1.99) into the Euler–Bernoulli equation given by Eq. (1.86) and realizing that the stiffness EI of the flexible member is constant, we find

$$\frac{y''}{\left[1 + (y')^2\right]^{3/2}} = \frac{w_0 x}{2EI} \int_0^x \left\{1 + [y'(x)]^2\right\}^{1/2} dx \tag{1.100}$$

Equation (1.100) is the exact nonlinear integral differential equation for the cantilever beam in Fig. 1.7, and its solution is again very difficult.

We can simplify, however, the solution of Eq. (1.100) by assuming that x_o in Eq. (1.97) is given by Eq. (1.74). We rewrite this equation for convenience:

$$x_0(x) = x + \Delta(x) \tag{1.101}$$

Reasonable expressions to use for the horizontal displacement $\Delta(x)$ in Eq. (1.101), are given by Eqs. (1.81)–(1.84). If we decide to use Eq. (1.81), where the horizontal displacement Δ of the free end B of the flexible member is assumed to remain constant, then Eq. (1.101) yields

$$x_0(x) = x + \Delta \tag{1.102}$$

By substituting Eq. (1.102) into Eq. (1.97), we find

$$M_x = -\frac{w_0 x}{2}(x + \Delta) \tag{1.103}$$

and the Euler–Bernoulli nonlinear differential equation yields,

$$\frac{y''}{\left[1 + (y')^2\right]^{3/2}} = \frac{w_0 x}{2EI}(L - \Delta) \tag{1.104}$$

The solution of Eq. (1.104) is by far the most convenient to use when it is compared to Eq. (1.100)

If we make the assumption that $\Delta(x)$ is given by Eq. (1.82), then Eq. (1.101) yields

$$x_0(x) = x + \frac{\Delta x}{L_0} \tag{1.105}$$

and the expression for the bending moment given by Eq. (1.97), becomes

$$M_x = -\frac{w_0 x}{2}\left(x + \frac{\Delta x}{L_0}\right) \tag{1.106}$$

Therefore, by substitution, the Euler–Bernoulli equation yields

$$\frac{y''}{\left[1 + (y')^2\right]^{3/2}} = \frac{w_0 x}{2EI}\left(x + \frac{\Delta x}{L_0}\right) \tag{1.107}$$

Again, the nonlinear differential equation given by Eq. (1.107) is much simpler to solve, compared to the integral nonlinear differential equation given by Eq. (1.100). Similar simplifications are obtained by using Eq. (1.83) or Eq. (1.84) for the function $\Delta(x)$.

1.8 General Theory of the Equivalent Systems for Linear and Nonlinear Deformations

In the preceding sections it was shown that the solution of the Euler–Bernoulli differential equation becomes extremely difficult when the deformation of the member under consideration is large, and when the stiffness variation and loading conditions along its length vary arbitrarily. For flexible members, that is members which are subjected to large deformation, even simple cases of loading and constant stiffness will complicate a great deal the solution of the flexible problem.

In this section *the theory of the equivalent systems*, as it was developed by the author and his collaborators [2, 3, 5, 6, 15, 18], will be developed here for both linear and nonlinear problems. The emphasis, however, is concentrated in the solution of nonlinear problems, because this is the purpose of this text. For more information on linear systems the reader may consult the work of the author in [6, 84], as well as in other references at the end of this book.

The theory of the equivalent systems is general, and it applies to many structural problems which incorporate arbitrary variations of loading and moment of inertia along the length of a member, as well as variations of the modulus of elasticity of its material. The modulus of elasticity variations that are extensively examined in later sections of this book are the ones produced by large loadings that cause the material of the member to be stressed beyond its elastic limit and all the way to failure. In such cases, the modulus E will vary along the length of the member.

The purpose of the theory of the equivalent systems is to provide a much simpler mathematical model, in terms of *pseudolinear equivalent systems* and simplified *nonlinear equivalent systems*, that can be used to solve the extremely complicated nonlinear problem with well known simple methods of

linear analysis. The pseudolinear equivalent system will always have a uniform stiffness EI throughout its equivalent length, and its loading will be different from the one acting on the original system. In other words, the length and loading of the pseudolinear equivalent system will be different, but its response will be identical to that of the original system.

1.8.1 Nonlinear Theory of the Equivalent Systems: Derivation of Pseudolinear Equivalent Systems

The derivation of pseudolinear equivalent systems of constant stiffness EI may be initiated by employing the Euler–Bernoulli law of deformations given by Eqs. (1.7) and (1.16). We rewrite Eq. (1.16) as follows:

$$\frac{y''}{\left[1+(y')^2\right]^{3/2}} = -\frac{M_x}{E_x I_x} \tag{1.108}$$

where the bending moment M_x, the modulus of elasticity E_x and the moment of inertia I_x are assumed to vary in any arbitrary manner.

The curvature of the member represented by the left-hand side of Eq. (1.108) is geometrical in nature, and it requires that the parameters M_x, E, and I on the right-hand side of the same equation to be also associated with the deformed configuration of the member. When the loading on the member is distributed and/or the cross-sectional moment of inertia is variable, the expressions for these parameters are in general nonlinear integral equations of the deformation and contain functions of horizontal displacement. That is, the bending moment M_x, depth h_x of the member, and moment of inertia I_x are all functions of both x and x_o. This is easily observed by examining the deformed configuration of the doubly tapered cantilever beam in Fig. 1.8. Therefore, the bending moment M_x has to be defined with respect to the deformed segment. On the other hand, the total load acting on an undeformed segment of a member does not change after the segment is deformed.

The variable stiffness $E_x I_x$, as discussed earlier, may be expressed as

$$E_x I_x = E_1 I_1 g(x) f(x) \tag{1.109}$$

where g(x) represents the variation of E_x with respect to a reference value E_1, and f(x) represents the variation of I_x with respect to a reference value I_1. If the member has a constant modulus of elasticity E and a constant moment of inertia I throughout its length, then g(x) = f(x) =1.00, and $E_x I_x$ = EI. In this case, the constant stiffness EI becomes the reference stiffness value $E_1 I_1$

By substituting Eq. (1.109) into Eq. (1.108), we have

$$\frac{y''}{\left[1+(y')^2\right]^{3/2}} = -\frac{1}{E_1 I_1}\,\frac{M_x}{g(x) f(x)} \tag{1.110}$$

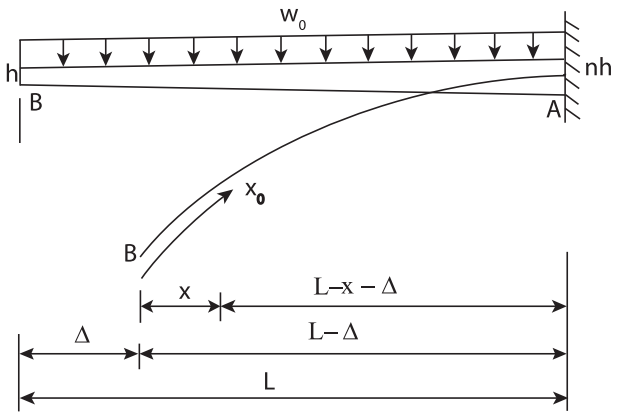

Fig. 1.8. Doubly tapered cantilever beam loaded with a uniformly distributed load w_o

If we integrate, hypothetically, Eq. (1.110) twice, the expression for the large transverse displacement y may be written schematically as

$$y(x) = \frac{1}{E_1 I_1} \int \left\{ - \int \left[1 + (y')^2 \right]^{3/2} \frac{M_x dx}{g(x) f(x)} \right\} dx + C_1 \int dx + C_2 \quad (1.111)$$

where C_1 and C_2 are the constants of integration which can be determined by using the boundary conditions of the member.

If we consider a member that has a constant stiffness $E_1 I_1$ and with an identical length and reference system of axes with the one used for Eq. (1.111), then we can write the expression for its large deflection y_e as follows:

$$y_e = \frac{1}{E_1 I_1} \int \left\{ - \int \left[1 + (y_e')^2 \right]^{3/2} M_e dx \right\} dx + C_1' \int dx + C_2' \quad (1.112)$$

In Eq. (1.112), M_e is the bending moment at any cross section x, and C_1' and C_2' are the constants of integration.

On this basis, the deflection curves expressed by y and y_e in Eqs. (1.111) and (1.112), respectively, will be identical if

$$C_1 = C_1' \quad \text{and} \quad C_2 = C_2' \quad (1.113)$$

$$\int \left\{ - \int \left[1 + (y')^2 \right]^{3/2} \frac{M_e dx}{f(x) g(x)} \right\} dx = \int \left\{ - \int \left[1 + (y_e')^2 \right]^{3/2} M_e dx \right\} dx \quad (1.114)$$

The conditions imposed by Eq. (1.113) are easily satisfied if the two members have the same arc length and boundary conditions. Equation (1.114) will be satisfied if $y_e' = y'$ and

$$M_e = \frac{M_x}{f(x) g(x)} \quad (1.115)$$

By following this way of thinking and examining Eq. (1.114), we conclude that the identity given by Eq. (1.114) will be satisfied when

$$\left[1+(y_e')^2\right]^{3/2} M_e = \left[1+(y')^2\right]^{3/2} \frac{M_x}{f(x)\,g(x)} \tag{1.116}$$

When the deformation of the members is small, then the angular rotations $(y')^2$ and $(y_e')^2$ may be neglected as being small compared to 1, and Eq. (1.116) reduces to Eq. (1.115). Thus, for small deflections, the moment diagram M_e of the equivalent system of constant stiffness E_1I_1 can be obtained from Eq. (1.115). Its equivalent shear force V_e and equivalent loading w_e can be obtained from Eq. (1.115) by differentiation. That is,

$$V_e = \frac{d}{dx}(M_e) = \frac{d}{dx}\left[\frac{M_x}{f(x)\,g(x)}\right] \tag{1.117}$$

$$w_e = -\frac{d}{dx}(V_e)\cos\theta = -\frac{d^2}{dx^2}\left[\frac{M_x}{f(x)\,g(x)}\right]\cos\theta \tag{1.118}$$

where $\cos\theta \approx 1$ when the rotations θ of the member are small. The equivalent constant stiffness system in this case is linear, and linear small deflection theory can be used for its solution.

When the deflections and rotations are large, $(y')^2$ and $(y_e')^2$ in Eqs. (1.110) and (1.116) cannot be neglected. By examining these two equations we observe that the moment M_e' of the equivalent pseudolinear system of constant stiffness E_1I_1 should be obtained from the equation

$$M_e' = \left[1+(y')^2\right]^{3/2} M_e = \left[1+(y')^2\right]^{3/2} \frac{M_x}{f(x)\,g(x)} = \frac{z_e}{f(x)\,g(x)} M_x \tag{1.119}$$

where

$$z_e = \left[1+(y')^2\right]^{3/2} \tag{1.120}$$

Also we note that $\theta = \tan^{-1}(y')$ represents the slope of the initial nonlinear system.

By solving Eq. (1.110) for y'', we obtain

$$y'' = -\frac{1}{E_1I_1}\left[1+(y')^2\right]^{3/2} \frac{M_x}{f(x)\,g(x)} \tag{1.121}$$

By substituting Eqs. (1.115) and (1.120) in Eq. (1.121) we find

$$y'' = \frac{M_e'}{E_1I_1} \tag{1.122}$$

Equation (1.122) is a pseudolinear differential equation and represents the pseudolinear equivalent system of constant stiffness E_1I_1. Therefore, it can be

treated and solved as a linear differential equation once the moment diagram $M_e{}'$ of the pseudolinear equivalent system is known.

The shear force $V_e{}'$ and loading $w_e{}'$ of the equivalent constant stiffness pseudolinear system may be determined from the expressions

$$V_e{}' = \frac{d}{dx}\left(M_e{}'\right) = \frac{d}{dx}\left[1 + (y')^2\right]^{3/2} M_e = \frac{d}{dx}\left[\frac{z_e}{f(x)\, g(x)}\right] M_x \tag{1.123}$$

$$\begin{aligned} w_e{}' &= -\frac{d}{dx}\left(V_e{}'\right)\cos\theta = \frac{d^2}{dx^2}\left[1 + (y')^2\right]^{3/2} M_e \cos\theta \\ &= -\frac{d^2}{dx^2}\left[\frac{z_e}{f(x)\, g(x)}\right] M_x \cos\theta \end{aligned} \tag{1.124}$$

When the equivalent constant stiffness pseudolinear system is obtained, elementary linear deflection theory and methods can be used to solve it. This is appropriate, because the deflections and rotations obtained by solving the pseudolinear system are identical to those of the original nonlinear system.

It should be also noted at this point that the equivalent moment diagram M_e given by Eq. (1.115), represents the moment M_e at any point x of a nonlinear equivalent system of length L equal to that of the original nonlinear system and of constant stiffness E_1I_1. This proves that we can also obtain equivalent simplified nonlinear systems by using Eq. (1.115). Consequently, the linearization of the initial variable stiffness flexible member, is obtained by multiplying M_e by the expression $\left[1 + (y')^2\right]^{3/2}$, as shown in Eq. (1.119). This is an extremely important observation, because, as it is shown later in this text, many complicated nonlinear problems with complex loadings and stiffness variations can be solved conveniently by obtaining first a simpler nonlinear equivalent system of constant stiffness E_1I_1 and then use it to proceed with pseudolinear analysis to obtain a pseudolinear equivalent system. This approach is amply illustrated in later parts of the text. Note also that V_e and w_e in Eqs. (1.117) and (1.118), respectively, give the shear force and loading, respectively, of the nonlinear equivalent system of constant stiffness E_1I_1.

We can simplify a great deal the mathematics regarding the computation of $V_e{}'$ and $w_e{}'$, or V_e and w_e, by approximating the shape of the moment diagram represented by Eq. (1.119), or the one represented by Eq. (1.115), with a few straight lines judiciously selected. This approximation simplifies to a large extent the derivation of pseudolinear and simplified nonlinear equivalent systems of constant stiffness. On this basis, the loading on the pseudolinear, or the equivalent linear system, will always consist of concentrated loads. This approach is amply illustrated in the following example.

Example 1.4 Determine a pseudolinear equivalent system for the uniform flexible cantilever beam of Example 1.1. By using the pseudolinear system determine the deflection and rotation at the free end. Show also how deflections and rotations can be determined at other points along the length of the member.

Solution: In Example 1.1, it was found that the horizontal displacement Δ of the flexible cantilever beam in Fig. 1.1a is 183.10 in. (4.65 m). The function G(x), in terms of Δ, is given by Eq. (1.65). By substituting the value of Δ into this equation, we find

$$\begin{aligned} \mathrm{G}\,(\mathrm{x}) &= 1.111\,(10)^{-6}\left[\mathrm{x}^2 - (1{,}000 - 183.10)^2\right] \\ &= 1.111\,(10)^{-6}\left[\mathrm{x}^2 - 667{,}325.61\right] \end{aligned} \tag{1.125}$$

From Eq. (1.67), the expression for $\mathrm{y}'(\mathrm{x})$ is

$$\mathrm{y}'\,(\mathrm{x}) = \frac{\mathrm{G}\,(\mathrm{x})}{\left\{1 - [\mathrm{G}\,(\mathrm{x})]^2\right\}^{1/2}} \tag{1.126}$$

and from Eq. (1.119), the moment diagram M'_{e} of the pseudolinear equivalent system can be determined from the expression

$$\mathrm{M}'_{\mathrm{e}} = \mathrm{z_e M_x} = \left[1 + (\mathrm{y}')^2\right]^{3/2} \mathrm{M_x} \tag{1.127}$$

where $\mathrm{M_x}$, is the bending moment at any location x of the original system. The values of y' can be determined by using Eqs. (1.125) and (1.126). Note that $\mathrm{g(x)} = \mathrm{f(x)} = 1, \mathrm{EI} = 180 \times 10^3$ kip in.^{2}(516.54×10^3 N m^2), P = 0.4 kip (1.78 kN) and L = 1,000 in. (25.4 m).

The bending moment $\mathrm{M_x}$ at any x between zero and $\mathrm{L_o} = \mathrm{L} - \Delta = 816.9$ in. (20.75 m), may be obtained from the equation

$$\mathrm{M_x} = -\mathrm{Px} = 0.4\mathrm{x} \tag{1.128}$$

Table 1.1 provides the calculated values of G(x), $\mathrm{y}'(\mathrm{x})$, $\mathrm{z_e}, \mathrm{M_x}$ and M'_{e} at various positions x between zero and 816.9 in. (20.75 m). By using the values of $\mathrm{M_e}'$ in the last column of Table 1.1, we plot the moment diagram M'_{e} of the pseudolinear system as shown in Fig. 1.9a. We approximate the *shape* of $\mathrm{M_e}'$ by four straight lines as shown in the same figure. The juncture points of these four straight lines may be located on above, or below the $\mathrm{M_e}'$ curve, represented by the solid line in Fig. 1.9a. The purpose here is to approximate the shape of the $\mathrm{M_e}'$ curve so that the areas added to this diagram and the areas subtracted from this diagram approximately balance each other. This can be done judiciously without any computations, because the accuracy of the calculated rotations and deflections depends mostly upon retaining the general shape of the $\mathrm{M_e}'$ curve during its approximation with straight lines, but they are not very sensitive as to how accurately this approximation is performed. Even with moderately large errors in the approximation of $\mathrm{M_e}'$, we obtain, for practical purposes, reasonable values for deflections and rotations. The reason for this is that, mathematically you get from moment to rotation and then to deflection by integration. When an appreciable error is introduced in the moment diagram curve, it reduces substantially by the time it gets to

Table 1.1. Values of G(x), $y'(x)$, z_e, M_x and $M_e'(x)$ at various locations $0 \le x \le 816.9$ in.(1 in. = 0.0254 m, 1 kip in. = 113 N m, 1 kip = 4.448 kN)

(1) x (in.)	(2) G(x) Eq. (1.125)	(3) $y'(x)$ Eq. (1.126)	(4) z_e Eq. (1.120)	(5) M_x (kip in.) Eq. (1.128)	(6) M_e' (kip in.) Eq. (1.127)
0	−0.7414	−1.1049	3.3095	0	0
100.0	−0.7303	−1.0689	3.1361	−40.00	−125.44
200.0	−0.6970	−0.9720	2.7121	−80.00	−216.97
300.0	−0.6414	−0.8360	2.2144	−120.00	−265.73
400.0	−0.5636	−0.6822	1.7739	−160.00	−283.82
500.0	−0.4636	−0.5232	1.4375	−200.00	−287.50
600.0	−0.3414	−0.3632	1.2043	−240.00	−289.03
700.0	−0.1970	−0.2009	1.0611	−280.00	−297.12
800.0	−0.0304	−0.0304	1.0014	−320.00	−320.45
816.9	0	0	1.000	−326.76	−326.76

rotation and deflection. This point was extensively investigated by the author and his students.

By applying statics, the shear force diagram is plotted as shown in Fig. 1.9b. For example,

$$V_1 = \frac{-170 - 0}{136.9} = -1.2418 \text{ kip } (5.5235 \text{ kN})$$
$$V_2 = \frac{-280 - (-170)}{200} = -0.55 \text{ kip } (2.4464 \text{ kN})$$

and so on. The *equivalent pseudolinear system* has length $L_o = L - \Delta = 816.9$ in. (20.75 m), and the loading is as shown in Fig. 1.9c. The loading is obtained by using Fig. 1.9b and applying statics. For example,

$$P_1 = 1.2418 \text{ kip } (5.5235 \text{ kN}) \quad \text{(downward)}$$
$$P_2 = 1.2418 - 0.55 = 0.6918 \text{ kip } (3.0771 \text{ kN}) \quad \text{(upward)}$$

and so on.

The pseudolinear system in Fig. 1.9c is, for practical purposes, an excellent approximation of the original nonlinear system. Linear methods of analysis, or available formulas from handbooks, may be used to solve the pseudolinear system for rotations and deflections. For example, the deflection and rotation at the free end B of the original system in Fig. 1.1a, may be determined by using the pseudolinear system in Fig. 1.9c and calculating its rotation and deflection at B' by using handbook formulas, or known methods of basic mechanics, such as the moment–area method. Superposition is permissible, because the pseudolinear system is linear.

In order to use the moment–area method, we divide the M_e' diagram in Fig. 1.9a by the constant stiffness $EI = 180 \times 10^3$ kip in.^{2}(516.54×10^3 N m^2)

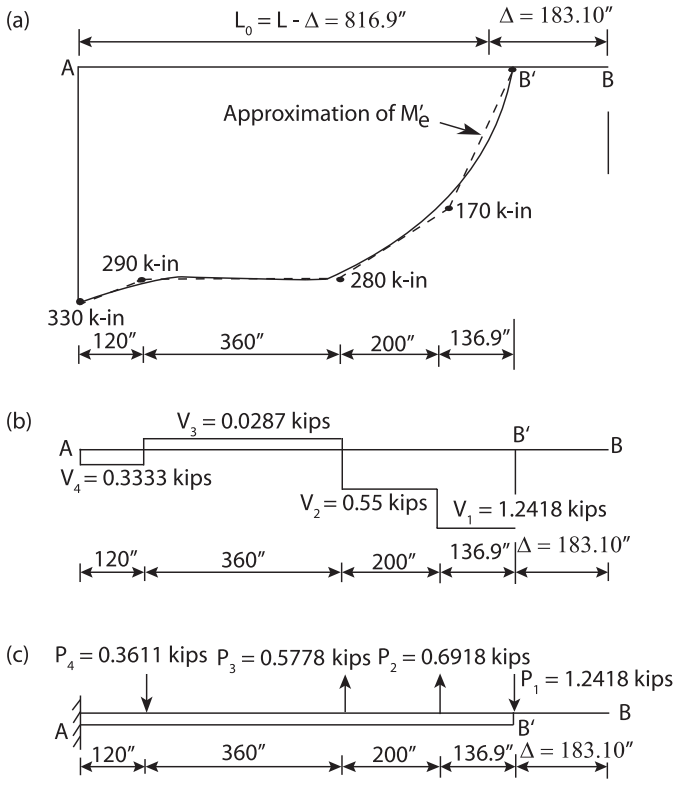

Fig. 1.9. (**a**) Moment diagram M_e' of the pseudolinear system with its shape approximated with four straight lines. (**b**) Shear force diagram. (**c**) Equivalent pseudolinear system of length $L_o = L - \Delta = 816.9$ in. (1 in. = 0.0254 m, 1 kip in. = 113 N m, 1 kip = 4.448 kN)

to obtain the M_e'/EI diagram. The deflection $\delta_{B'}$ at the free end B′ of the pseudolinear system is equal to the first moment of the M_e'/EI diagram between A and B′, taken about B′. By using the straight-line approximation of M_e' shown by the dashed lines in Fig. 1.9a, dividing it by EI and then taking its first moment about B′, we find

$$\begin{aligned}\delta_{B'} &= \frac{1}{EI}\left[\frac{1}{2}(170)(136.9)\left(\frac{2}{3}\right)(136.9) + (170)(200)(236.9)\right.\\ &\quad +\frac{1}{2}(110)(200)(270.2333) + (280)(360)(516.9) + \frac{1}{2}(10)(360)(576.9)\\ &\quad \left.+(290)(120)(756.9) + \frac{1}{2}(40)(120)(776.9)\right]\\ &= \frac{1}{EI}[98, 170, 244]\end{aligned}$$

or

$$\delta_{B'} = \frac{1}{180(10)^3}[98, 170, 244] = 545.39 \text{ in. } (13.85 \text{ m})$$

Also, by using the moment–area method, $y_{B'}{}'$ at the free end of the pseudolinear system would be equal to the total $M_e{}'/EI$ area between points A and B′. Thus, by using again Fig. 1.9a, we obtain

$$\begin{aligned} y_{B'}{}' &= \frac{1}{EI}\left[\frac{1}{2}(170)(136.9) + (170)(200) + \frac{1}{2}(110)(200) + (280)(360)\right. \\ &\qquad \left. + \frac{1}{2}(10)(360) + (290)(120) + \frac{1}{2}(40)(120)\right] \\ &= \frac{1}{EI}[196, 436.5] \end{aligned}$$

or

$$y_{B'}{}' = \frac{1}{180(10)^3}[196, 436.5] = 1.0913$$

Thus,

$$\theta_{B'} = \tan^{-1}(y_B{}') = 47.50^\circ$$

The calculated values $\delta_{B'}$ and $\theta_{B'}$ that were obtained by using the pseudolinear system in Fig. 1.9c are very accurate, at least for practical applications, and they are closely identical to the analogous exact values at the end B that can be obtained by solving directly the original member in Fig. 1.1a. In fact, the direct solution was obtained by integrating directly the Euler–Bernoulli equation given by Eq. (1.46). On this basis we found that the deflection and rotation at the end B of the nonlinear member in Fig. 1.1a, are $\delta_B = 523.27$ in. (13.29 m) and $\theta_B = 47.86^\circ$. If we can assume that these last two values are the exact values, then the error by using the pseudolinear system would be 4.22% for the deflection and 0.75% for the rotation. However, if it is required, the accuracy can be improved if we will approximate the moment diagram of the pseudolinear system, shown in Fig. (1.9a), with more straight lines. The purpose in using the pseudolinear system is to simplify the solution of complicated nonlinear problems with complicated loading conditions and moment of inertia variations. This point of view is clearly demonstrated throughout this text.

By using direct integration, Table 1.2 has been prepared which shows the variation of δ_B, Δ_B, and θ_B at the free end B of the flexible beam for the indicated values of the concentrated vertical load P at the free end B. The second column of the table gives the values of δ_B that were obtained by neglecting y' and proceeding with linear analysis. If we compare these values with the analogous ones shown in the third column of the table, we note that the error by using linear analysis becomes unreasonably huge as the load P increases, and such linear procedures should not be used for flexible members.

By using nonlinear analysis, the large deflection configurations of the flexible member for values of the load $P = 1, 3$, and 10 kip, are shown plotted

Table 1.2. Values of δ_B, Δ_B, and θ_B for various values of P and comparisons with linear theory (1 in. = 0.0254 m, 1 kip = 4.448 kN)

load P	linear analysis	nonlinear analysis		
(kips)	δ_B (in.)	δ_B (in.)	Δ_B (in.)	θ_B (deg.)
0.2	370.37	328.61	67.36	28.90
0.4	740.74	523.27	183.10	47.86
0.6	1,111.11	629.00	281.29	59.42
0.8	1,481.48	691.58	356.71	66.87
1.0	–	732.14	414.95	71.95
2.0	–	821.37	577.22	83.23
2.5	–	841.64	621.12	85.48
3.0	–	856.20	653.84	86.92
5.0	–	888.86	731.69	89.00
10.0	–	921.40	810.27	89.61

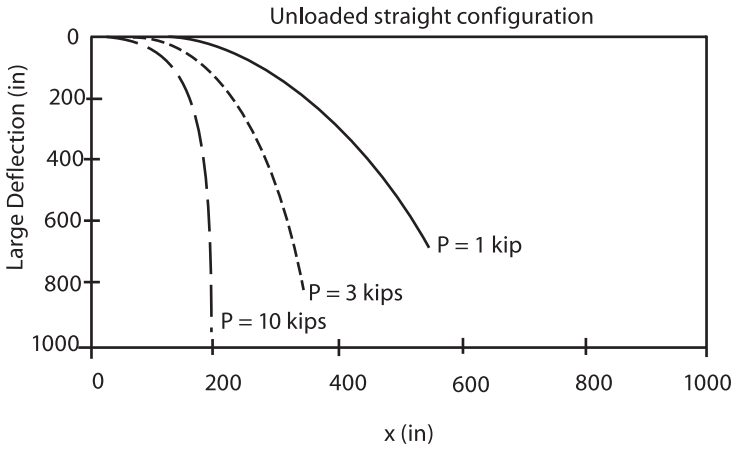

Fig. 1.10. Large deflection curves for P = 1, 3, and 10 kip (1 kip = 4.448 kN, 1 in. = 0.0254 m)

in Fig. 1.10. Note that for P = 10 kip (44.48 kN), the member is practically hanging in the vertical direction.

Deflections and Rotations at Any x Between Zero and L_o

We can also use the pseudolinear system in Fig. 1.9c to determine the vertical deflection y and rotation y' at any $0 \leq x \leq L_o$. Since this system is now linear, we can use any linear method of analysis, or existing handbook formulas to do it. For this problem, the moment–area method and handbook formulas are convenient to use. Since the pseudolinear system is linear, superposition can be used. That is, if you prefer, you can solve the pseudolinear system in Fig. 1.9c for each concentrated vertical load separately and superimpose the results.

It should be pointed out, however, that the length L_o of the pseudolinear system is not equal to the length L of the original system, and the same applies for the values of x and x_o. The pseudolinear system provides the values y and y' at any $0 \le x \le L_o$, but for each x there corresponds a value of $0 \le x_o \le L$, where L is the length of the original member, which can be determined from Eq. (1.75). We rewrite this equation below:

$$x_0(x) = \int_0^x \left\{1 + [y']^2\right\}^{1/2} dx \tag{1.129}$$

The Simpson's rule given by Eq. (1.36) in Sect. 1.5 can be used for this purpose.

Let it be assumed, for example, that we used the pseudolinear system in Fig. 1.9c, we then applied the moment–area method, and we determined the values of y and y' at $x = 100$ in. (2.54 m), and we want to know the value of x_o of the original system in Fig. 1.1a that corresponds to $x = 100$ in. (2.54 m). We can do this by using Simpson's One-Third rule.

If we use this rule and assume $n = 10$, then Eq. (1.70) yields

$$\lambda = \frac{100 - 0}{10} = 10 \tag{1.130}$$

By examining Eq. (1.29), we note that the function f(x) to be used in Eq. (1.69), is

$$f(x) = \left\{1 + [y'(x)]^2\right\}^{1/2} dx \tag{1.131}$$

The values of f(x) at $x = 0, 10, 20, \ldots, 100$, are designed as $y_o, y_1, \ldots, y_{10}$, respectively, and they are determined by using Eq. (1.131) in conjunction with Eqs. (1.65) and (1.67), which are as follows:

$$G(x) = 1.111(10)^{-6}[x^2 - 667,325.61] \tag{1.132}$$

$$y'(x) = \frac{G(x)}{\{1 - [G(x)]^2\}^{1/2}} \tag{1.133}$$

For example, at $x = 0$, we have

$$\begin{aligned} G_0 &= -0.783922 \\ y'(0) &= \frac{-0.783922}{\sqrt{1 - (-0.783922)^2}} = -1.262641 \\ y_0 &= f(0) = \sqrt{1 + (-1.262641)^2} = 1.610671 \end{aligned}$$

At $x = 10$ in. (0.254 m), we have

$$\begin{aligned} G(10) &= 1.111(10)^{-6}[10^2 - 667,325.61] = -0.741288 \\ y'(10) &= \frac{-0.741288}{\sqrt{1 - (-0.741288)^2}} = \frac{-0.741288}{0.671188} = -1.104442 \\ y_1 &= f(10) = \sqrt{1 + (-1.104442)^2} = 1.489896 \end{aligned}$$

In a similar manner, the remaining values of $y_2, y_3, \ldots, y_{10}$, are determined.

By substituting into Eq. (1.69), we find

$$\begin{aligned} x_0 = \frac{10}{3}\,&[1.610671 + (4)(1.489896) + (2)(1.489079) + (4)(1.487724) \\ &+(2)(1.485832) + (4)(1.483413) + (2)(1.480479) \\ &+(4)(1.477039) + (2)(1.473105) + (4)(1.468699) + 1.463833] \\ = \frac{10}{3}&[44.558578] = 148.53 \text{ in. } (3.77 \text{ m}) \end{aligned}$$

Therefore, we can conclude that when we calculate the deflection or the rotation of the equivalent pseudolinear system at x = 100 in. (2.54 m), the corresponding position x_o on the original nonlinear system is 148.53 in. (3.77 m). In other words, there is a complete mathematical correspondence between x and x_o which defines the nature of the pseudolinear equivalent system. It should be also pointed out that the deflection curve of the equivalent pseudolinear system is identical to the one of the original nonlinear system.

1.8.2 Nonlinear Theory of the Equivalent Systems: Derivation of Simplified Nonlinear Equivalent Systems

It was stated earlier that the large deformations of flexible members are no longer a linear function of the bending moment or of the applied load and, consequently, the principle of superposition is not applicable. This restriction creates enormous difficulties when we try to solve beam problems with more elaborate loading conditions. The solution becomes even more complicated when the moment of inertia of a flexible member varies arbitrarily along its length. The flexible cantilever beam in Fig. 1.11, loaded as shown, illustrates a mild case of an elaborate combined loading condition coupled with a variable depth along the length of the member. A reasonable solution to such types of problems can be obtained if a simpler equivalent mathematical model is first obtained that accurately (or exactly) represents the initial complicated mathematical problem. This may be accomplished by reducing the initial nonlinear problem into a simpler equivalent nonlinear problem that can be solved more

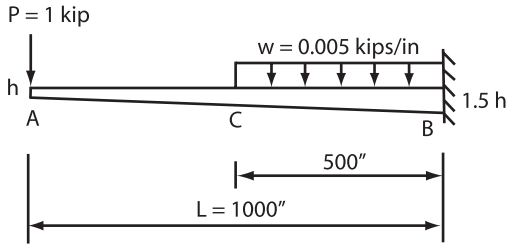

Fig. 1.11. Tapered flexible cantilever beam loaded as shown

conveniently by using either pseudolinear analysis as discussed earlier, or by utilizing available solutions (or solution methodologies) of nonlinear analysis.

The derivation of constant stiffness nonlinear equivalent systems, can be carried out by using Eq. (1.108) and substituting for the variable stiffness E_xI_x the expression given by Eq. (1.109), yielding

$$\frac{y''}{[1+(y')^2]^{3/2}} = -\frac{1}{E_1I_1}\frac{M_x}{g(x)f(x)} \tag{1.134}$$

or

$$\frac{y''}{[1+(y')^2]^{3/2}} = -\frac{M_e}{E_1I_1} \tag{1.135}$$

where

$$M_e = \frac{M_x}{g(x)f(x)} \tag{1.136}$$

Equation (1.135) is the nonlinear differential equation of an equivalent system of constant stiffness E_1I_1, whose bending moment M_e at any cross section is given by Eq. (1.136). Therefore, the variable stiffness nonlinear system represented by Eq. (1.134), and the one of constant stiffness represented by Eq. (1.135), will have identical deflection curves. Therefore, we can conclude that Eq. (1.135) may be used to solve the variable stiffness problem by applying nonlinear analysis. In order to make the solution easier, the shape of the M_e diagram represented by Eq. (1.136) may be approximated with a few straight lines. This procedure will produce a simpler constant stiffness equivalent nonlinear system that is always loaded with a few concentrated loads as it was accomplished earlier for the pseudolinear system.

The following example illustrates the application of the theory and methodology.

Example 1.5 The tapered flexible cantilever beam in Fig. 1.12a is loaded with a distributed triangular load $w_o = 0.01$ kip in.$^{-1}$(1,751.27 N m^{-1}), and a concentrated vertical load $P = 1$ kip (4.448 kN) at its free end. At the free end B the stiffness $EI_B = 180 \times 10^3$ kip in.^{2}(516,551 N m^2). Determine a simplified nonlinear equivalent system of constant stiffness EI_B. The width of the member is constant and equal to b, and the modulus of elasticity E is constant.

Solution: The depth h_x at any distance x from the free end B of the member is given by the equation

$$h_x = h\left(1+\frac{x}{2L}\right) \tag{1.137}$$

Therefore, for rectangular cross sections, the moment of inertia I_x at any distance x from the end B of the member is

$$I_x = \frac{bh_x^3}{12} = \frac{bh^3}{12}\left[1+\frac{x}{2L}\right]^3 = I_Bf(x) \tag{1.138}$$

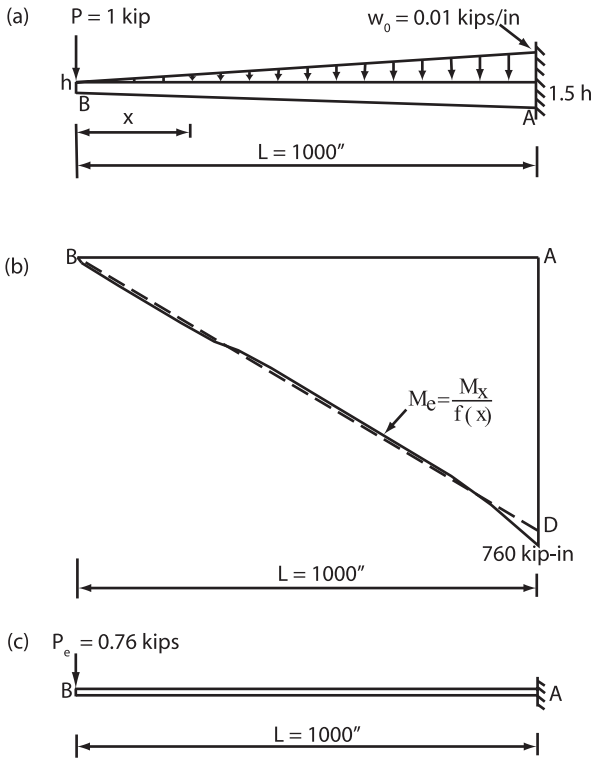

Fig. 1.12. (**a**) Original tapered cantilever beam loaded as shown. (**b**) Moment diagram M_e of the simplified nonlinear equivalent system of constant stiffness EI_B. (**c**) Simplified nonlinear equivalent system (1 in. = 0.0254 m, 1 kip = 4,448 N, 1kip in. = 113 N m)

where h_x is given by Eq. (1.137) and

$$I_B = \frac{bh^3}{12} \tag{1.139}$$

$$f(x) = \left[1 + \frac{x}{2L}\right]^3 \tag{1.140}$$

The moment diagram M_e of the simplified nonlinear equivalent system of constant stiffness EI_B, can be obtained by using Eq. (1.136). In this equation the modulus function g(x) is constant and equal to one. In the same equation, the moment M_x at any distance x from the free end B of the member, can be determined by using the original member in Fig. 1.12a and applying statics. For convenience, Table (1.3) has been prepared, where the first column of the table shows the selected values of x, the second column gives the corresponding values of f(x) using Eq. (1.140), the third column gives the values of M_x which are determined by applying statics, and the last column of the table gives

Table 1.3. Values of f(x), M_x and M_e for the indicated values of x (1 in. = 0.0254 m, 1 kip in. = 113 N m)

(1) x (in)	(2) f(x)	(3) M_x (kip-in)	(4) $M_e = \frac{M_x}{f(x)}$ (kip in.)
0	1	0	0
100	1.1576	−101.67	−87.83
200	1.3310	−213.33	−160.28
300	1.5209	−345.00	−226.84
400	1.7280	−506.67	−293.21
500	1.9531	−708.33	−362.67
600	2.1970	−960.00	−436.96
700	2.4604	−1,271.67	−516.85
800	2.7440	−1,653.33	−602.44
900	3.0486	−2,115.00	−693.76
1,000	3.3750	−2,666.67	−790.12

the values of M_e at the selected values of x, which are obtained by using Eq. (1.136).

The M_e diagram is plotted as shown by the solid line in Fig. 1.12b. A very reasonable approximation of this diagram would be the straight dahed line BD drawn as shown in the same figure. By using the straight line approximation and applying statics, we obtain the simplified nonlinear equivalent system of uniform stiffness EI_B shown in Fig. 1.12c. This system is a great deal simpler when we compare it to the original system in Fig. 1.12a. To solve the simplified nonlinear system we can use the pseudolinear analysis discussed earlier in this section Example 1.4. We can also do it by direct integration of the Euler–Bernoulli equation given by Eq. (1.135), or by using tables which are prepared using elliptic integral solution and are available in the literature [85].

In [85, p. 516], a table is provided by the author that can be used to determine the horizontal, vertical, and rotational displacements at the free end of a uniform flexible cantilever beam, loaded by a vertical concentrated load P at the free end. The solution is based on elliptic integrals, and provides reliable answers for practical applications. By using this table we find that at the free end of the simplified nonlinear equivalent system shown in Fig. 1.12c, we have, $\theta_B = 65.46^o$, vertical displacement $\delta_B = 679.78$ in. (17.27 m), and horizontal displacement $\Delta_B = 342.11$ in. (8.69 m).

In order to compare results, the original system in Fig. 1.12a was solved by the author and his students by deriving its Euler–Bernoulli nonlinear differential equation based on $x_o = x + \Delta$, where Δ is the horizontal displacement of its free end B. Then this equation was integrated twice to determine the vertical deflection at the free end B. The two constants of integration were determined by using the boundary conditions of zero rotation and zero deflection at the fixed end, and the required integrations were carried out by using Simpson's rule. The result obtained was $\delta_B = 701.0$ in. (17.81 m), giving

a difference of 3.02%. The same problem was also solved by using the Runge–Kutta method, yielding $\theta_B = 67.54°$, a difference of 3.08%, and $\delta_B = 708.00$ in. (17.99 m), a difference of 4.0%. We note that all these approaches provided reliable results, but the use of simplified nonlinear equivalent systems is by far the simplest method to use.

Other cases of such problems can be treated in a similar manner. We should always remember that even with very crude approximations of the moment diagram with straight line segments, we will always obtain a reasonable solution to the problem for practical applications. Some caution, however, should be taken to retain the general shape of the moment diagram during its approximation with straight line segments. The approximations shown in Figs. 1.9a and 1.12b are considered to be excellent, and good accuracy, for practical applications, could be obtained using even fewer straight line segments in Fig. 1.9a.

1.8.3 Linear Theory of the Equivalent Systems

When the deformations of a member in bending are small, the y' in Eq. (1.110) is small when it is compared to one and it can be neglected for practical applications. On this basis, Eq. (1.110) reduces to the following second order differential equation:

$$y'' = -\frac{1}{E_1 I_1} \frac{M_x}{f(x)g(x)} \tag{1.141}$$

Also, from Eq. (1.120), we find $z_e = 1.0$, and from Eq. (1.119) we find

$$M'_e = M_e = \frac{M_x}{f(x)g(x)} \tag{1.142}$$

Therefore, Eq. (1.141) can be written as

$$y'' = -\frac{M_e}{E_1 I_1} \tag{1.143}$$

where in this equation the moment M_e is given by Eq. (1.142).

Equation (1.142) provides the bending moment of a linear equivalent system of constant stiffness $E_1 I_1$ at any location x of the member. With known M_e, the equivalent shear force V_e and the equivalent loading w_e of the constant stiffness equivalent system can be obtained from Eq. (1.142) by differentiation. That is,

$$V_e = \frac{d}{dx}(M_e) = \frac{d}{dx}\left[\frac{M_x}{f(x)g(x)}\right] \tag{1.144}$$

$$w_e = -\frac{d}{dx}(V_e)\cos\theta = -\frac{d^2}{dx^2}\left[\frac{M_x}{f(x)g(x)}\right]\cos\theta \tag{1.145}$$

where $\cos\theta \approx 1$ when the rotations are small. For more information on this subject you may refer to the work of the author and his collaborators given in the references at the end of this book.

The following examples illustrate the application of the theory.

Example 1.6 A tapered cantilever beam of rectangular cross section is loaded by a vertical load P at the free end B, as shown in Fig. 1.13a. The depth h_x of the member, for convenience, is selected to be

$$h_x = \left(\frac{3L - 2x}{L}\right)^{1/3} h \tag{1.146}$$

If the deformations of the member are assumed to be small, determine an exact equivalent system of constant stiffness EI_B. Also determine an approximate

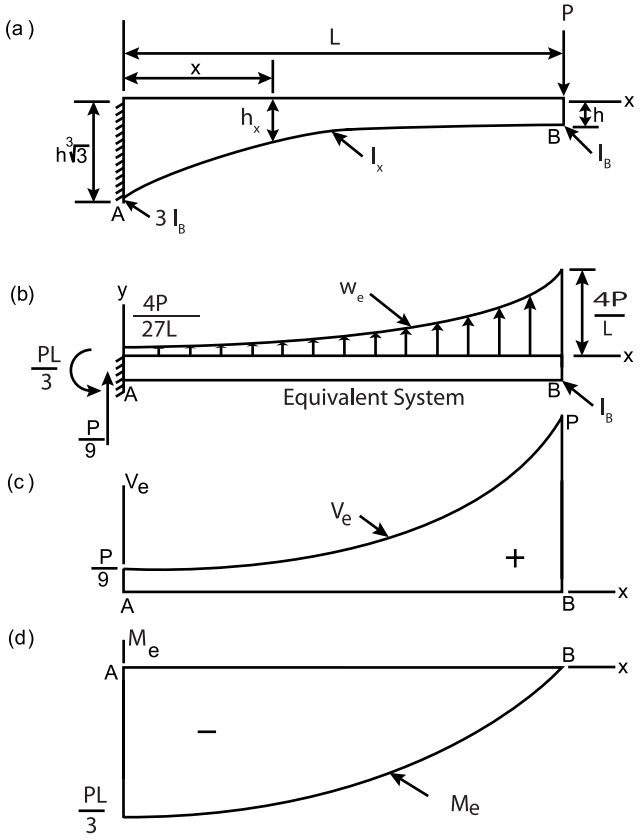

Fig. 1.13. (**a**) Tapered cantilever beam loaded as shown. (**b**) Exact equivalent system of constant stiffness EI_B. (**c**) Shear force diagram of the equivalent system. (**d**) Moment diagram M_e of the equivalent system

equivalent system loaded with vertical concentrated loads. The modulus of elasticity E and the width b of the member are constant.

Solution: For the assumed variation of h_x, the moment of inertia I_x of the member is

$$I_x = \frac{bh_x^3}{12} = \frac{3L - 2x}{L} \frac{bh^3}{12} = I_B f(x) \tag{1.147}$$

where

$$f(x) = \frac{3L - 2x}{L} \tag{1.148}$$

$$I_B = \frac{bh^3}{12} \tag{1.149}$$

At any x from the fixed end of the member, the bending moment M_x is

$$M_x = -P(L - x) \tag{1.150}$$

From Eq. (1.142), by substituting for f(x) which is given by Eq. (1.148) and noting that the function g(x) = 1, we find that the bending moment M_e of the equivalent system of constant stiffness EI_B is

$$M_e = \frac{M_x}{f(x)} = -\frac{PL(L - x)}{3L - 2x} \tag{1.151}$$

where M_x is given by Eq. (1.150).

By differentiating M_e once, we find the shear force V_e of the equivalent system, which is

$$V_e = \frac{dM_e}{dx} = \frac{PL^2}{(3L - 2x)^2} \tag{1.152}$$

Also, by differentiating V_e once, we obtain the loading w_e of the equivalent system of constant stiffness EI_B. That is

$$w_e = \frac{dV_e}{dx} = \frac{4PL^2}{(3L - 2x)^3} \tag{1.153}$$

Equations (1.151), (1.152), and (1.153) are plotted as shown in Figs. 1.13d, 1.13c, and 1.13b, respectively. Figure 1.13b illustrates the exact equivalent system of constant stiffness EI_B, loaded as shown, which produces a deflection curve that is identical to the deflection curve produced by the original system in Fig. 1.13a.

We proceed now with the second part of the problem which requires to determine an approximate equivalent system of constant stiffness EI_B which will be loaded with vertical concentrated loads.

An accurate approximation may be obtained by approximating the shape of M_e in Fig. 1.13d with a few straight-line segments, as it was done earlier for the nonlinear analysis. In order to get numerical results, we assume that

P = 10 kip (44,480 N) and L = 300 in. (7.62 m). On this basis, Eq. (1.151) yields

$$M_e = -\frac{1,500(300 - x)}{450 - x} \tag{1.154}$$

Equation (1.154), which represents the exact variation of the moment M_e of the equivalent system of constant stiffness EI_B, is plotted as shown by the solid line in Fig. 1.14a. In this figure, the shape of M_e is approximated with two straight-line segments as shown by the dashed line. By using statics we plot the shear force diagram as shown in Fig. 1.14b, and the simplified equivalent system of constant stiffness EI_B shown in Fig. 1.14c. If we solve the approximate equivalent system in Fig. 1.14c, we will find out that its deflections and rotations are closely identical to those of the original system in

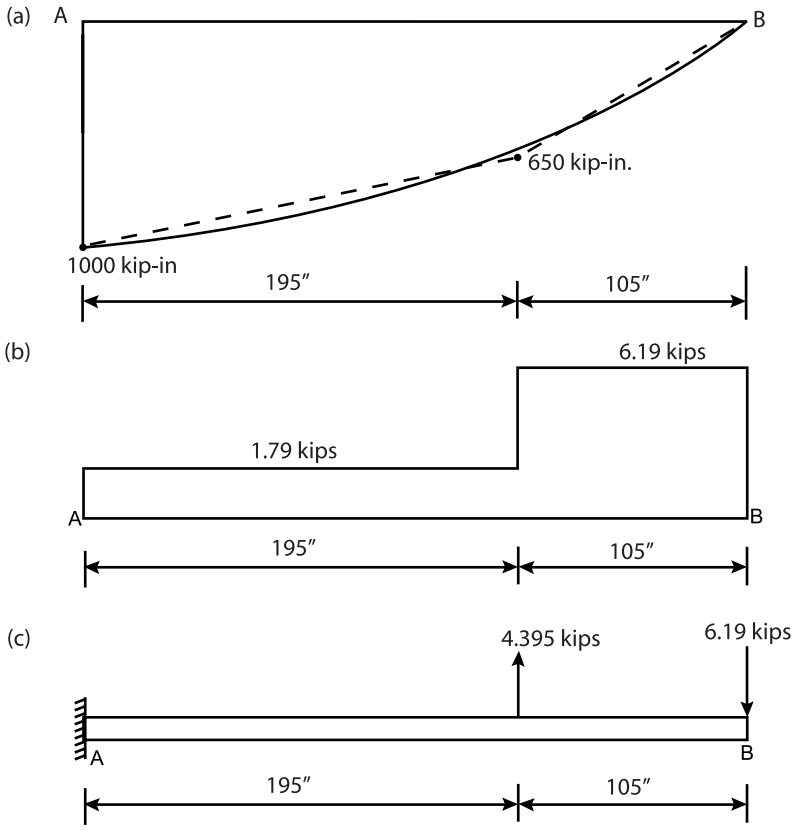

Fig. 1.14. (**a**) M_e diagram with its shape approximated with two straight-line segments. (**b**) Shear force diagram V_e. (**c**) Approximate equivalent system of constant stiffness EI_B loaded with two concentrated loads as shown (1 in. = 0.0254 m, 1 kip = 4, 448 N, 1 kip in. = 112.9848 N m)

Fig. 1.13a and to those of the exact equivalent system in Fig. 1.13b. However, the solution of the approximate equivalent system in Fig. 1.14c is very simple when it is compared to the solution of the systems in Fig. 1.13a and 1.13b.

By using the approximate equivalent system in Fig. 1.14c and applying the moment–area method, we find that the deflection δ_B at the free end B is $105,022.44/EI_B$, and the rotation θ_B at the same end is $999.975/EI_B$ radians. The units of E and I_B are kip in.$^{-2}$ and in.^{4}, respectively. Compared to the exact solution, the error by using the two straight-line approximation for M_e, would be less than 1.5% for the deflection, and much less for the rotation. However, if required, we can improve the accuracy by using more straight-line segments for the approximation of M_e.

Example 1.7 A simply supported rectangular stepped beam of variable cross section, is loaded as shown in Fig. 1.15a. By approximating the shape of the M_e diagram with straight-line segments, determine an approximate equivalent system of uniform stiffness EI_I, where I_I, is the moment of inertia of the member at its end B. The width b of the member and its modulus E are constant.

Solution: At various locations x, where x is measured from the left support A, the values of M_x, f(x), and M_e are calculated and they are shown in Table 1.4. The moment diagram M_x of the original system in Fig. 1.15a, is plotted in Fig. 1.15c using the values of M_x in Table 1.4. The variation f(x) of the moment of inertia I_x in terms of I_1, where I_1 is the moment of inertia at the end B, is plotted as shown in Fig. 1.15b.

By using the values of $M_e = M_x/f(x)$ shown in the last column of Table 1.4, the moment diagram M_e of the equivalent system of constant stiffness EI_1 is shown plotted by the solid line in Fig. 1.16a. The shape of the M_e diagram is now approximated with four straight-line segments as shown by the dashed line in the same figure. By applying statics, using the approximated M_e diagram, we plot the equivalent shear force diagram shown in Fig. 1.16b. By

Table 1.4. Calculated values of M_x, f(x), and M_e at various locations x from the left support A (1 ft = 0.3048 m, 1 kip ft = 1,355.75 N m)

x (ft)	M_x (kip ft)	f(x)	$M_e = M_x/f(x)$ (kip ft)
0	0	17.560	0
5	37.5	13.820	2.71
10	50.0	10.650	4.69
10	50.0	2.745	18.22
12	48.0	2.300	20.85
14	42.0	1.908	22.00
15	37.5	1.728	21.70
18	18.0	1.260	14.27
20	0	1.000	0

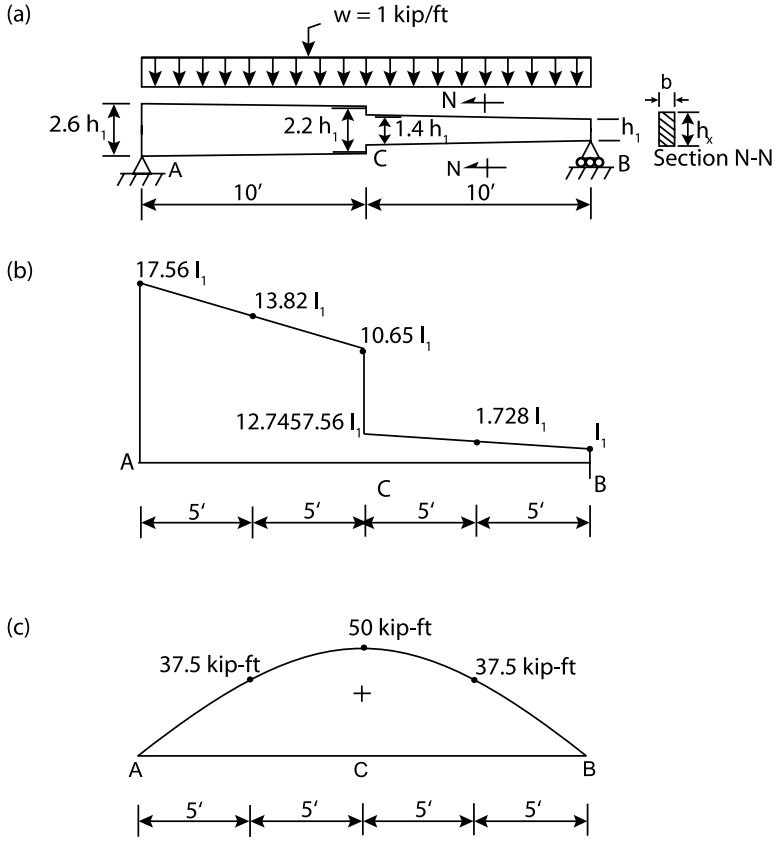

Fig. 1.15. (**a**) Simply supported stepped beam of variable stiffness. (**b**) Moment of inertia variation. (**c**) Moment diagram M_x of the initial system in Fig. 1.15a. (1 ft = 0.3048 m, 1 kip ft^{-1} = 14,593 N m^{-1}, 1 kip ft = 1,355.75 N m)

using this shear force diagram and applying static, we obtain the approximate equivalent system of constant stiffness EI_1 shown in Fig. 1.16c.

Note that in addition to the concentrated vertical loads, a concentrated moment equal to 12.72 kip ft (18.22 − 5.5 = 12.72) (16,990.74 N m) must also act at point C of the equivalent system in Fig. 1.16c. This is justified because in this case there is an abrupt change of the bending moment M_e at point C. This means that a step in the original system in Fig. 1.15a requires a concentrated moment at the analogous point of the uniform stiffness equivalent system, in order to compensate for the elimination of the step.

By using the equivalent system in Fig. 1.16, deflections and rotations can be determined by using linear methods of analysis or handbook formulas.

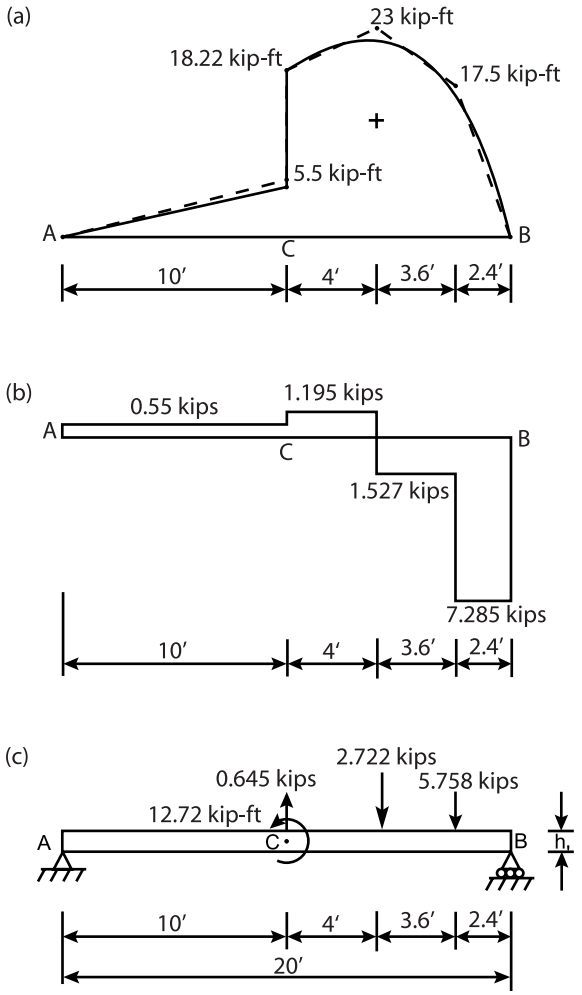

Fig. 1.16. (**a**) Moment diagram M_e with its shape approximated with four straight-line segments. (**b**) Equivalent shear force diagram. (**c**) Equivalent system of constant stiffness EI_1 (1 ft = 0.3048 m, 1 kip ft = 1,335.75 N m)

These rotations and deflections will be closely identical with the ones at corresponding points of the original system in Fig. 1.15a.

Example 1.8 The depth d_x and the moment of inertia variation I_x of the elastically supported beam in Fig. 1.17a, are

$$d_x = (\frac{L+3x}{L})^{1/3} d_1 \tag{1.155}$$

$$I_x = \frac{L+3x}{L} I_1 = f(x) I_1 \tag{1.156}$$

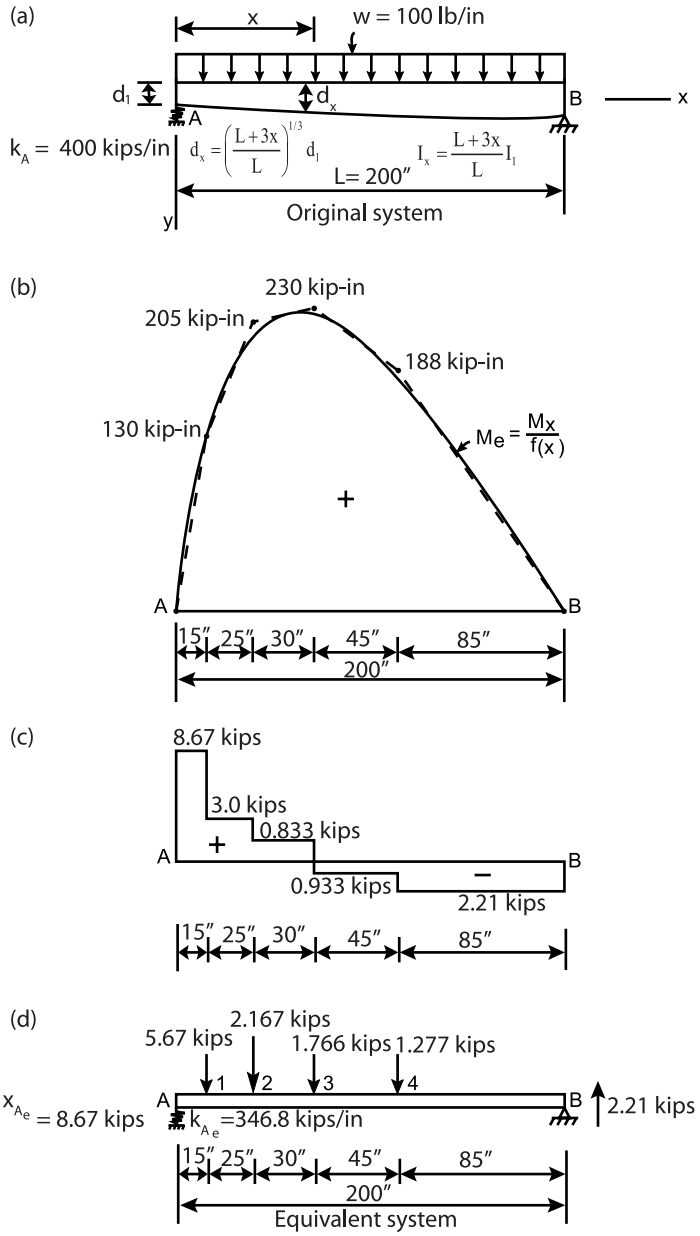

Fig. 1.17. (**a**) Original variable stiffness member. (**b**) M_e diagram with its shape approximated with five straight-line segments. (**c**) Equivalent shear force diagram. (**d**) Equivalent system of constant stiffness EI_1(1 ft = 0.3048 m, 1 kip = 4, 448.222 N, 1 kip in. = 113 N m, 1 in. = 0.0254 m, 1 lb in^{-1} = 175.118 N m^{-1})

where d_1 is the depth of the member at support A, $I_1 = bd_1^3/12$ (where b is the constant width of the member), is the moment of inertia at support A, and x is measured from support A. The modulus of elasticity E of the member is constant, the stiffnesss $EI_1 = 90 \times 10^6$ kip in.^{2}, and at support A the spring stiffness $k_A = 400$ kip in^{-1} (70,050.74 kN). Determine the equivalent system of constant stiffness EI_1. The length L = 200 in. (5.08 m).

Solution: If x_A is the elastic reaction from the spring at support A, then by considering the free body diagram of the beam and taking moments about the end point B, we obtain

$$\sum M_B = -200X_A + (100)(200)(100) = 0$$
$$X_A = 10 \text{ kip in. } 44,482.22$$

The values of f(x), M_x, and $M_e = M_x/f(x)$ are calculated at various positions x from support A, and they are as shown in Table 1.5.

The values of M_e given in the last column of Table 1.5 are used to plot the M_e diagram shown by the solid line in Fig. 1.17b. The shape of M_e is then approximated in the usual way with five straight-line segments as shown in the same figure. Note the values of the approximated M_e at the juncture points of the straight-line segments. Using these values of the approximated M_e and applying statics, we determine the equivalent shear force diagram shown in Fig. 1.17c. From the equivalent shear force diagram in Fig. 1.17c, by using statics, we determine the equivalent system of constant stiffness EI_1, shown in Fig. 1.17d.

There is however, an additional boundary condition at support A that must be satisfied. At this support, the vertical displacement δ_A of the spring of stiffness k_A in Fig. 1.17a, must be equal to the vertical displacement δ_{A_e} of the spring of stiffness k_{A_e} of the equivalent system in Fig. 1.17d. We know that

$$\delta_A = \frac{X_A}{k_A} \tag{1.157}$$

Table 1.5. Values of f(x), M_x, and M_e at various positions x from support A (1 in. = 0.0254 m, 1 kip in. = 113 N m)

x (in.)	f(x)	M_x (kip in.)	$M_e = M_x/f(x)$ (kip in.)
0	1.000	0	0
25	1.375	218.8	159.0
50	1.750	375.0	214.0
75	2.125	468.0	221.0
100	2.500	500.0	220.0
125	2.875	468.0	163.0
150	3.250	375.0	115.0
175	3.625	218.8	60.4
200	4.000	0	0

and

$$\delta_{A_e} = \frac{X_{A_e}}{k_{A_e}} \tag{1.158}$$

Thus, from Eqs. (1.157) and (1.158), for $\delta_A = \delta_{A_e}$, we must have

$$\frac{X_A}{k_A} = \frac{X_{A_e}}{k_{A_e}} \tag{1.159}$$

Thus, Eq. (1.159) yields

$$k_{A_e} = k_A \frac{X_{A_e}}{X_A} \tag{1.160}$$

By using again statics, the elastic reaction X_{A_e} of the equivalent spring at support A of the equivalent system in Fig. 1.17d, was found to be equal to 8.67 kip (38,566.085 N). On this basis, Eq. (1.160) yields

$$k_{A_e} = (400)\frac{8.67}{10} = 346.8 \text{ kip in.}^{-1}(60.731 \times 10^6 \text{ N m}^{-1})$$

Now the derivation of the equivalent system of constant stiffness EI_1 is completed and shown in Fig. 1.17d. The elastic line of this system will be practically identical to the one of the original system in Fig. 1.17a. The only approximation we have introduced is the approximation of the M_e diagram with five straight-line segments as shown in Fig. 1.17b. If you observe this diagram closely, you note that its general shape is well retained and, therefore, the error we introduce to the actual deflections and rotations is very small. Even a two- or a three-line approximation would give very reasonable results for practical applications.

By using the equivalent system in Fig. 1.17d and applying the conjugate beam method, we find that the vertical deflection at the distance x = 70 in. (0.778 m) from support A is 0.02542 in. (0.000646 m). The exact value is 0.02535 in. (0.000644 m), yielding an error of 0.28%. For practical purposes this error is considered to be negligible. In many cases, much higher errors are permissible for practical applications.

Example 1.9 A statically indeterminate tapered beam made out of steel is loaded as shown in Fig. 1.18a. The width b of the member is 6 in. (0.1524 m), and the depth h = 10 in. (0.254 m). By applying the method of the equivalent systems, determine the vertical reaction at support A. The constant modulus of elasticity $E = 30 \times 10^6$ psi (206.84×10^9 Pa).

Solution: The variation of the depth h_x at any distance x from support A is

$$h_x = h(1 + \frac{x}{L}) \tag{1.161}$$

and the expression for the variation of the moment of inertia I_x is

$$I_x = \frac{bh_x^3}{12} = I_A(1 + \frac{x}{L})^3 \tag{1.162}$$

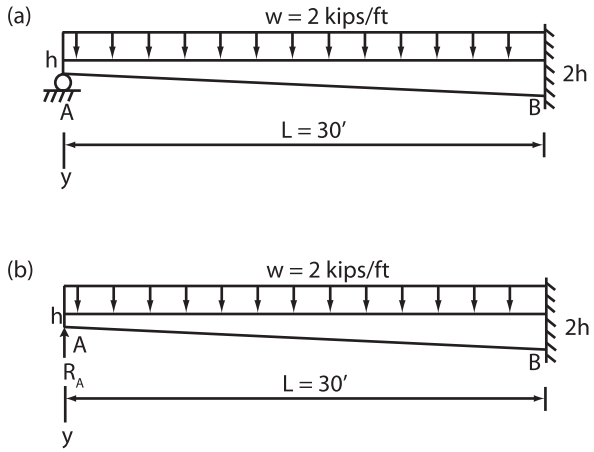

Fig. 1.18. (**a**) Tapered statically indeterminate steel beam. (**b**) Tapered cantilever beam loaded with the distributed loading and the redundant reaction R_A at the free end A ($1\,\text{ft} = 0.3048\,\text{m}, 1\ \text{kip ft}^{-1} = 14,593.18\,\text{Nm}^{-1}$)

or

$$I_x = I_A f(x) \tag{1.163}$$

where

$$I_A = \frac{bh^3}{12}$$

is the moment of inertia at the left support A, and

$$f(x) = (1 + \frac{x}{L})^3 \tag{1.164}$$

represents the variation of the moment of inertia I_x.

Since the beam is statically indeterminate, the reaction R_A at the support A is taken as the redundant quantity. On this basis, we now have a cantilever beam loaded with the distributed load w and the reaction R_A as shown in Fig. 1.18b. The linear method of the equivalent systems may be applied here by using the cantilever beam in Fig. 1.18b and deriving two equivalent systems– one by using only R_A as the applied loading, and a second one by using only the distributed load w as the applied load.

The procedure is illustrated in Table 1.6. The first column of the table includes selected values of x, the second column gives the values of f(x) at these points, the third column gives the values of M_x produced only by the application of R_A, and the fourth column shows the values of the moment M_e of the equivalent system of constant stiffness EI_A produced by the application of R_A. The fifth column of the table gives the values of M_x produced only by the application of the distributed load w, and the last column of the table gives the values of the moment M_e of the equivalent system of constant stiffness EI_A produced by the application of the load w. The reader may verify the values in the table in order to become familiar with the methodology.

Table 1.6. Values of f(x), M_x, and M_e caused independently by the reaction R_A and loading w, for the cantilever beam in Fig. 1.18b (1 ft = 0.3048 m, 1 kip ft = 1,355.75 N m, 1 kip ft^{-1} = 14,593.18 N m^{-1})

(1) x (ft)	(2) f(x)	(3) M_x due to R_A (kip ft)	(4) M_e due to R_A (kip ft)	(5) M_x due to w (kip ft)	(6) M_e due to w (kip ft)
0	1.0000	0	0	0	0
5	1.5880	5 R_A	3.1486 R_A	−25	−15.7431
10	2.3704	10 R_A	4.2187 R_A	−100	−42.1870
15	3.3750	15 R_A	4.4444 R_A	−225	−66.6667
20	4.6296	20 R_A	4.3200 R_A	−400	−86.4006
25	6.1620	25 R_A	4.0571 R_A	−625	−101.4281
30	8.0000	30 R_A	3.7500 R_A	−900	−112.5000

By using the values of M_e in the fourth column of Table 1.6, the equivalent moment diagram M_e for the reaction R_A is plotted as shown in Fig. 1.19a. The approximation of its shape with four straight-line segments leads to the equivalent system for R_A shown in Fig. 1.19c. In a similar manner, by using the values of M_e in the last column of the table, the equivalent moment diagram M_e for the distributed load w is shown plotted in Fig. 1.20a. The approximation of its shape with three straight-line segments leads to the equivalent system for w shown in Fig. 1.20c.

If we use the equivalent systems in Figs. 1.19c and 1.20c and determine each time the vertical displacements δ_A' and δ_A'', respectively, the vertical reaction R_A at the support A of the original system in Fig. 1.18a may be determined by satisfying the boundary condition

$$\delta_A = \delta_A' + \delta_A'' = 0 \tag{1.165}$$

where δ_A is the deflection at A of the original system, which is zero.

The deflection δ_A' may be determined by applying the moment–area method. It can be accomplished by using the approximated M_e in Fig. 1.19a, dividing it by EI_A, and taking the first moment of the M_e/EI_A area between points A and B, about point A. On this basis, we find

$$\begin{aligned}
\delta_A' &= \left[\frac{1}{2}(3R_A)(4)\left(\frac{2}{3}\right)(4) + (3R_A)(6)(7)\right. \\
&\quad + \frac{1}{2}(1.4R_A)(6)(8) + (4.4R_A)(10)(15) \\
&\quad \left. + \frac{1}{2}(0.65R_A)(10)(23.3333) + (3.75R_A)(10)(25)\right](25)^3 \\
&= \frac{1}{EI_A}\left[16R_A + 126R_A + 33.6R_A + 600R_A + 75.8332R_A + 937.5R_A\right](12)^3 \\
&= \frac{1,848.93R_A}{EI_A}(12)^3
\end{aligned}$$

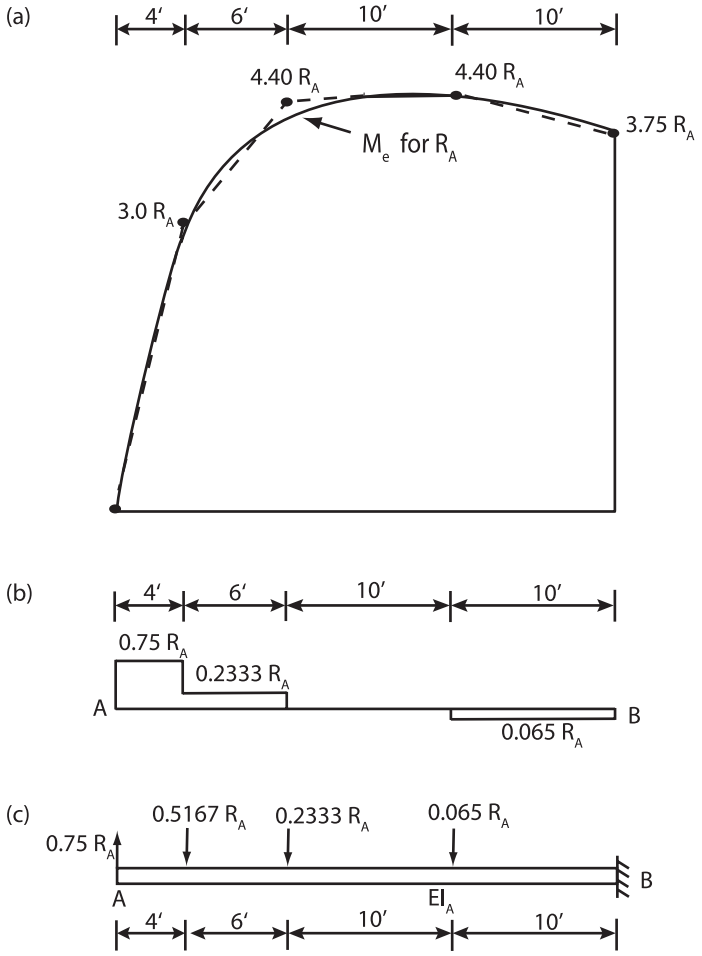

Fig. 1.19. Equivalent system for R_A. (**a**) M_e diagram with its shape approximated with four straight-line segments. (**b**) Equivalent shear-force diagram. (**c**) Equivalent system of constant stiffness EI_A(1 ft = 0.3048 m)

In a similar manner, by using the approximated M_e diagram in Fig. 1.120a, dividing it by EI_A, and taking its first moment about A, we find

$$\begin{aligned}\delta_A'' &= -\frac{1}{EI_A}\left[\frac{1}{2}(25)(7)\left(\frac{2}{3}\right)(7) + (25)(12)(13) + \frac{1}{2}(60)(12)(15)\right.\\ &\qquad \left. +(85)(11)(24.5) + \frac{1}{2}(27.5)(11)(26.3333)\right](12)^3\\ &= -\frac{35,271.11}{EI_A}(12)^3\end{aligned}$$

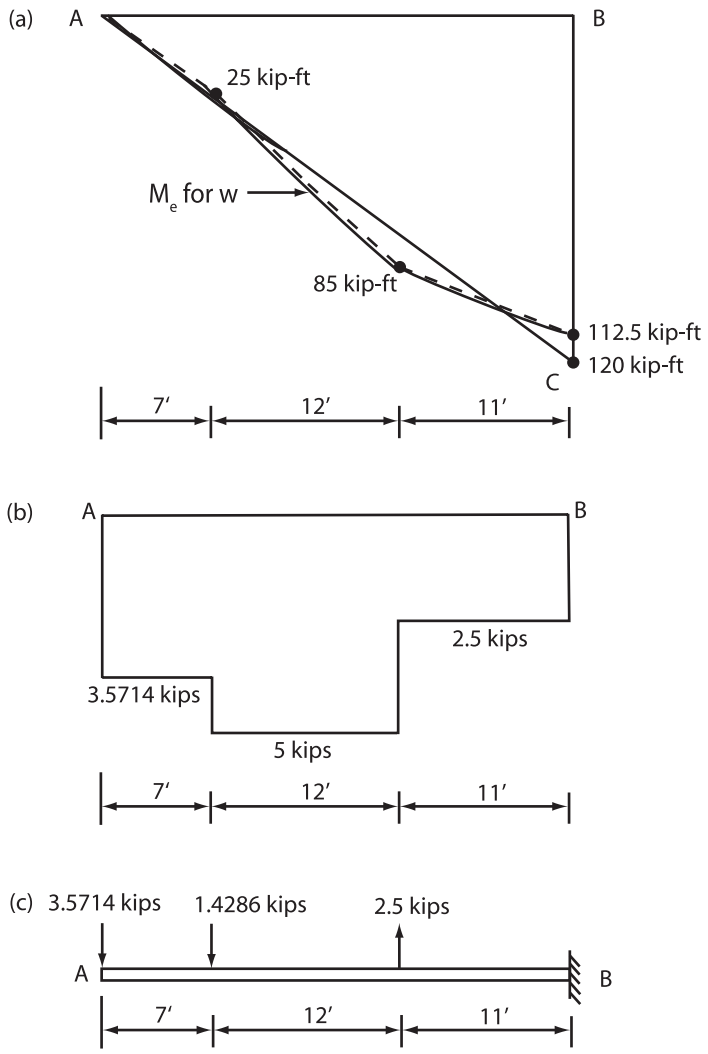

Fig. 1.20. Equivalent system for distributed load w. (**a**) M_e diagram with its shape approximated with three straight-line segments. (**b**) Equivalent shear-force diagram. (**c**) Equivalent system of constant stiffness EI_A (1 ft = 0.3048 m, 1 kip ft = 1, 355.75 N m, 1 kip = 4, 448 N)

By substituting the values of δ_A' and δ_A'' into Eq. (1.165) and solving for R_A, we find

$$\frac{1,848.93R_A}{EI_A}(12)^3 - \frac{35.271.11}{EI_A} = 0$$

or

$$R_A = 19.08 \text{ kip } (84.85 \times 10^3 \text{ N})$$

The value of R_A obtained here by using the indicated approximations for M_e should be very accurate–well within one percent. Better accuracy may be obtained by using more straight lines to approximate M_e.

Very reasonable results may be obtained even with crude approximations of the shape of M_e. For example, the approximation of the M_e diagram in Fig. 1.20a with one straight line AC, yields

$$\begin{aligned}\delta_A'' &= \frac{1}{EI_A}\left[\frac{1}{2}(120)(30)(20)\right](12)^3 \\ &= -\frac{36{,}000}{EI_A}(12)^3\end{aligned}$$

If it is compared to the value obtained earlier by using three straight-line segments, we find that the difference in δ_A'' is only 2.07%, and the difference in R_A would be 2.04%. Similar accuracy may be obtained if we approximate the M_e in Fig. 1.19a with two or three straight-line segments instead of four.

Other problems of this nature may be solved in a similar manner. See also [2, 3, 5, 6, 84] at the end of this text.

Problems

1.1 By using Simpson's One-Third rule, evaluate the integrals

$$\delta = \int_0^{20} (x+1)^2 dx, \qquad \delta = \int_0^{20} (x-5)^2 dx,$$
$$\delta = \int_0^{100} \frac{\sqrt{x}}{2} dx, \qquad \delta = \int_0^{100} (\frac{\sqrt{x}}{2})^3 dx$$

1.2 Repeat Example 1.1 by assuming that P = 0.6 kip (2.67 kN) and compare the results.
Answer: $\Delta_B = 281.29$ in. (7.145 m), $\theta_B = 59.42°$.

1.3 Repeat Example 1.1 by assuming that P = 1.4 kip (6.23 kN) and compare the results.
Answer: $\Delta_B = 557.22$ in. (14.66 m), $\theta_B = 83.23°$.

1.4 Repeat Example 1.2 by assuming that the beam in Fig. 1.6 has a uniform cross section throughout its length and compare the results.

1.5 Repeat Example (1.3) by assuming that $\Delta(x)$ is given, (a) by Eq. (1.83), and (b) by Eq. (1.84). Compare the results.

1.6 For the uniform flexible beam shown in Fig. 1.1a, determine a pseudolinear system of constant stiffness EI. Assume that P = 0.6 kip (2.67 kN), L = 1,000 in. (25.4 m), and EI = 180×10^3 kip n^2(516.54×10^3 N m^2). By using the pseudolinear system, determine the rotation and vertical deflection at the free end B. Also determine the horizontal displacement of the free end B.
Answer: $\delta_B = 629.0$ in. (15.98 m), $\Delta_B = 281.29$ in. (7.145 m), and $\theta_B = 59.42°$.

1.7 By using the pseudolinear system derived in Problem 1.6, determine the rotations and vertical displacements at x = 100 in. (2.54 m) and x = 300 in. (7.62 m). Also determine what values of x_o, in the original system, correspond to the indicated values of x.

1.8 Repeat Problem 1.6 by assuming that P = 1 kip (4.448 kN) and compare the results.

1.9 The tapered cantilever beam in Fig. 1.6 is loaded with a concentrated load P = 2.5 kip (11.12 kN) at the free end. By using a pseudolinear equivalent system of constant stiffness, determine the vertical and horizontal displacements δ_B and Δ_B, respectively, at the free end B of the beam, as well as the rotation θ_B at the same end. The length L = 1,000 in. (25.4 m), $EI_B = 180{,}000$ kip in^2(516.54×10^3 N m^2), and taper n = 1.5.
Answer: $\delta_B = 720.82$ in. (18.31 m), $\Delta_B = 436.60$ in. (11.10 m), and $\theta_B = 78.44°$.

1.10 Repeat Problem 1.9 by assuming that P = 1.5 kip (6.67 kN), and compare the results.
Answer: $\delta_B = 622.75$ in. (15.82 m), $\Delta_B = 298.0$ in. (7.145 m), and $\theta_B = 65.86°$.

1.11 Repeat Problem 1.9 by assuming that taper n = 2 and P = 1 kip (4.448 kN). Compare the results.
Answer: $\delta_B = 334.47$ in. (8.50 m), $\Delta_B = 78.42$ in. (1.99 m), and $\theta_B = 36.14°$.

1.12 Solve Problem 1.9 by using a simplified nonlinear equivalent system of constant stiffness EI_B that is loaded with one equivalent concentrated load P_e at the free end B of the beam. Apply pseudolinear analysis to solve the simplified nonlinear equivalent system. Compare the results.

1.13 Solve Problem 1.9 with P = 2.0 kip (8.889 kN).

1.14 Solve Problem 1.9 with P = 1 kip (4.448 kN), and n = 1.80.
Answer: $\delta_B = 401.23$ in. (10.19 m), $\Delta_B = 113.26$ in. (2.88 m), and $\theta_B = 42.39°$.

1.15 Solve the problem in Example 1.5 by assuming that P = 1.5 kip (6.672 kN) and $w_o = 0.02$ kips in.$^{-1}$($3{,}502.54$ N m^{-1}).

1.16 The uniform flexible cantilever beam in Fig. P1.16 is loaded by two concentrated loads located as shown in the figure. Determine a simplified nonlinear equivalent system of constant stiffness that is loaded with only

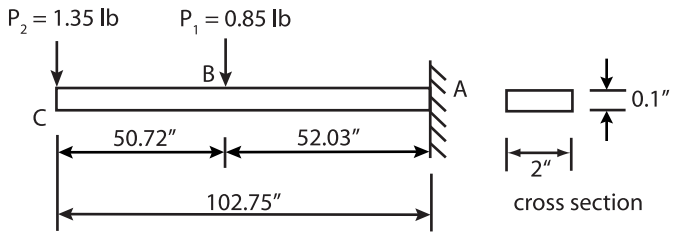

Fig. P1.16.

one concentrated equivalent vertical load at its free end C. The modulus of elasticity $E = 30 \times 10^6$ psi (206.84×10^6 kPa).

1.17 By using the simplified nonlinear equivalent system obtained in Problem 1.16 and applying pseudolinear analysis, determine the vertical deflection δ_C, the horizontal displacement Δ_C, and rotation θ_C, at its free end C. *Answer*: $\delta_C = 68.84$ in. (1.7485 m), $\Delta_C = 29.51$ in. (0.7496 m), and $\theta_C = 60°$ (1.0462 rad).

1.18 Repeat the problem in Example 1.6 by assuming that the length L = 600 in. (15.24 m) and compare the results.

1.19 Repeat the problem in Example 1.7 by assuming that w = 2 kips ft^{-1} (29, 186.36 N m^{-1}), and compare the results.

1.20 By using the constant stiffness equivalent system obtained in Example 1.7, determine the rotation θ_C and vertical displacement δ_C at midspan C of the member.

1.21 By using the constant stiffness equivalent system obtained in Example 1.8, determine its deflection and rotation at midspan.

1.22 Repeat the problem in Example 1.8 by assuming that w = 200 lb in.$^{-1}$ (35, 026 N m^{-1}).

1.23 Repeat the problem in Example 1.9 by assuming that w = 4 kips ft^{-1} (58, 372.72 N m^{-1}).

1.24 Repeat the problem in Example 1.8 by approximating the M_e diagram (a) with three straight-line segments, and (b) with only two straight-line segments appropriately selected. In each case, solve for the deflection and rotation at midspan and compare the results.

1.25 The variable stiffness steel beams in Fig. P1.25 are loaded as shown. The cross section of each member is rectangular with width b = 8 in.

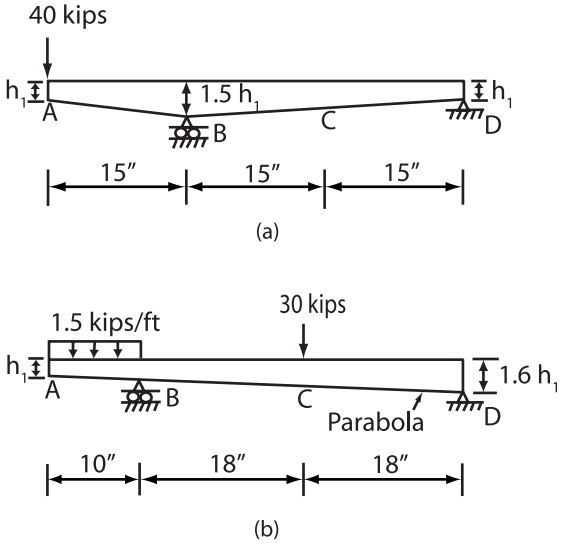

Fig. P1.25.

(0.2032 m) and depth $h_1 = 16$ in. (0.4064 m). By applying the linear theory of equivalent systems, determine in each case an equivalent system of uniform stiffness EI_A, where $E = 30 \times 10^6$ psi (206.84×10^9 Pa) is the constant modulus of elasticity, and I_A is the moment of inertia at the free end A. By using in each case the equivalent system, determine the vertical deflections at points A and C.

http://www.springer.com/978-3-540-32975-6

Nonlinear Structural Engineering
With Unique Theories and Methods to Solve Effectively
Complex Nonlinear Problems
Fertis, D.G.
2006, XIII, 339 p. 119 illus., Hardcover
ISBN: 978-3-540-32975-6